

On a pipeline pressure drop model for nonideal, compressible, gas mixture flow with application to pipeline flow of natural gas-hydrogen blends

Jeremy Conner, Vasilios I. Manousiouthakis*

Department of Chemical and Biomolecular Engineering,

University of California at Los Angeles (UCLA), Los Angeles, California, 90095

* Corresponding Author, Email: vasilios@ucla.edu, Phone: (310) 206-0300, 5549 Boelter Hall, Box 951592, Los Angeles, CA, 90095-1592

Abstract

This work presents a novel, dimensionless model that results in a dimensionless algebraic equation that can be used to quantify the pressure drop associated with the steady state, isothermal flow through a straight, horizontal pipeline, of a compressible gas mixture whose thermodynamic behavior is described for comparison purposes by ideal gas (IG) and nonideal gas generic cubic (GC) equation of state (EOS) models. A solution strategy, that uses the aforementioned dimensionless algebraic equation, is then presented that quantifies the pipeline pressure drop for hydrogen containing mixtures. Two case studies are presented to illustrate the pressure drop dependence on the hydrogen mole fraction of a binary, methane hydrogen mixture, and a natural gas hydrogen mixture with a real life natural gas composition containing eight species.

Notation

English Letters

$A_p(m^2)$: Pipeline cross section considered constant

$a(T)((J \cdot m^3)/(mol^2))$: Temperature dependent parameter of GCEOS

$b(m^3/mol)$: Parameter of GCEOS accounting for molecule finite size

$b^{IG}(m^3/mol) = \frac{b}{\Omega}$: Parameter accounting for molecule finite size, used in creating DIGEOS

$dl(m)$: Pipeline differential length

$d\hat{W}\left(\frac{m^2}{s^2}\right) = d\hat{W}\left(\frac{J}{kg}\right)$: Differential amount of work per unit mass provided to the gas mixture

$D_\beta \subset \mathbb{R}^+ \times \mathbb{R}^+$: Domain of (q, \tilde{V}) for DGCEOS

$D_p(m)$: Pipeline diameter considered constant

$D_p \subset \mathbb{R}^+ \times \mathbb{R}^+$: Domain of (T, V) for GCEOS

$f(\cdot)$: Friction factor of nonideal gas mixture

$k(J/K) = 1.380649 \cdot 10^{-23}$: Boltzmann constant

$l(m)$: Pipeline length running variable

$\tilde{l}(\cdot)$: Dimensionless pipeline length running variable

$L_p(m)$: Pipeline length

$\dot{m}\left(\frac{kg}{s}\right)$: mass flow rate

$m_i(kg\ i)$: mass of a single molecule of the i th species

$M\left(\frac{kg\ mix}{mol\ mix}\right)$: Molar mass of nonideal gas mixture

$M_{NG}\left(\frac{kg\ NG}{mol\ NG}\right)$: Molar mass of nonideal gas mixture

$M_i\left(\frac{kg\ i}{mol\ i}\right)$: i th species' molar mass

$N_A(1/mol) = 6.02214076 \cdot 10^{23}$: Avogadro number

$P(Pa)$: Pressure of nonideal gas mixture

$P_{c,i}(Pa)$: i th species' critical pressure

q : dimensionless temperature of nonideal gas mixture

$r_{KI} = \Omega^2 r_{KI}^{IG}$: dimensionless ratio of kinetic molar energy over internal molar energy for DGCEOS

r_{KI}^{IG} : dimensionless ratio of kinetic molar energy over internal molar energy for DIGEOS

r_{LD} : dimensionless ratio of pipeline diameter over pipeline length

$R(J/(mol \cdot K)) = 8.314$: Universal Gas Constant

$Re(\cdot)$: Reynolds number of gas mixture fluid flow

$R_h(m)$: Pipeline hydraulic radius considered constant

R_j : j th chemical reaction

S_i : i th species

$T(K)$: Temperature of nonideal gas mixture

$T_{c,i}(K)$: i th species' critical temperature

$T_{r,i}(K)$: i th species' reduced temperature

$T_i^*(\cdot)$: i th species' dimensionless temperature normalized by Lennard Jones potential parameter

$v\left(\frac{m}{s}\right)$: Gas mixture velocity

$v_0 \left(\frac{m}{s} \right)$: Gas mixture velocity at the pipeline entrance

$\tilde{v}(\cdot)$ Dimensionless velocity of gas mixture

$V \left(\frac{m^3 \text{ mix}}{\text{mol mix}} \right)$: Molar volume of nonideal gas mixture

$V_0 \left(\frac{m^3 \text{ mix}}{\text{mol mix}} \right)$: Molar volume of nonideal gas mixture at pipeline inlet

$\tilde{V}(\cdot) \triangleq \frac{V}{b}$: Dimensionless molar volume of gas mixture used in DGCEOS, normalized by the parameter b accounting for molecule finite size.

$\tilde{V}^{IG} \triangleq \frac{V}{b^{IG}} = \Omega \tilde{V}$ Dimensionless molar volume of gas mixture used in DIGEOS, normalized by the parameter b^{IG} accounting for molecule finite size.

$\tilde{V}_0(\cdot) \triangleq \frac{V_0}{b}$: Dimensionless molar volume of gas mixture normalized by GC EOS parameter b accounting for molecule finite size at pipeline inlet.

$\tilde{V}_0^{IG}(\cdot) \triangleq \frac{V_0}{b^{IG}} = \Omega \tilde{V}_0(\cdot)$: Dimensionless molar volume of gas mixture normalized by parameter b^{IG} accounting for molecule finite size at pipeline inlet.

$y_i \left(\frac{\text{mol } i}{\text{mol mix}} \right)$: ith species mole fraction

Z_c : compressibility factor at critical point

Greek Letters

$\alpha(T_{r,i}; \omega_i)(\cdot)$: Reduced temperature and acentric factor dependent parameter of GCEOS

$\beta \triangleq \frac{Pb}{RT}$: Dimensionless gas mixture pressure, normalized by temperature, used in DGCEOS

$\beta^{IG} \triangleq \frac{Pb^{IG}}{RT} = \frac{\beta}{\Omega}$ Dimensionless gas mixture pressure, normalized by temperature, used in DIGEOS

$\beta_0 \triangleq \frac{P_0 b}{RT}$: Dimensionless inlet gas mixture pressure, normalized by temperature, used in DGCEOS

$\beta_0^{IG} \triangleq \frac{P_0 b^{IG}}{RT} = \frac{\beta_0}{\Omega}$ Dimensionless inlet gas mixture pressure, normalized by temperature, used in DIGEOS

$\gamma(\cdot) : \mathbb{R}^+ \rightarrow \mathbb{R}$, $\gamma(\cdot) : \tilde{V} \rightarrow \gamma(\tilde{V})$: Dimensionless function of dimensionless molar volume used to express the mechanical energy balance. Its superscripts IG , GC refer to the IGEOS, GCEOS respectively, while 0σ , $\varepsilon\sigma$ refer to the relevant GCEOS respectively.

$\gamma_k(\cdot) : \mathbb{R}^+ \rightarrow \mathbb{R}$, $\gamma_k(\cdot) : \tilde{V} \rightarrow \gamma_k(\tilde{V})$, $k = 1, 2, 3$: Dimensionless components of dimensionless function of dimensionless molar volume used to express the mechanical energy balance.

$\Delta H_{f,i}^\circ \left(\frac{J}{mol \cdot i} \right)$: ith species' standard enthalpy of formation at temperature 298.15 K

$\varepsilon(\cdot)$: Model parameter for GCEOS

$\epsilon_i(J)$: Lennard Jones potential related parameter denoting the maximum energy of attraction between two molecules of the ith species

$\kappa(m)$: Constant defining pipeline roughness used in friction factor relations

$\mu(T) \left(\frac{kg \cdot mix}{m \cdot s} \right)$: Gas mixture viscosity that is a function of temperature

$\mu_i(T) \left(\frac{kg \cdot i}{m \cdot s} \right)$: Viscosity of ith species, that is considered to be a function of temperature

v_{ji} : Stoichiometric coefficient of the ith species in the jth chemical reaction

$\rho \left(\frac{kg \cdot mix}{m^3 \cdot mix} \right)$: Mass density of nonideal gas mixture

$\rho_0 \left(\frac{kg \cdot mix}{m^3 \cdot mix} \right)$: Mass density of nonideal gas mixture at pipeline inlet

$\rho_{0,CH_4}^{IG} \left(\frac{kg \cdot CH_4}{m^3} \right)$: Mass density of baseline CH₄ as ideal gas at pipeline inlet

$\rho_{0,CH_4} \left(\frac{kg \cdot CH_4}{m^3} \right)$: Mass density of baseline CH₄ gas at pipeline inlet

$\rho_{0,NG} \left(\frac{kg \cdot NG}{m^3} \right)$: Mass density of NG gas at pipeline inlet

$\sigma(\cdot)$: Model parameter for GC EOS

$\sigma_i \left(\overset{\circ}{A} \right)$: Collision diameter of Lennard Jones potential for ith species

$\Phi_{i,j}(\cdot)$: Dimensionless quantities used in the mixture viscosity semiempirical formula

$\Psi(\cdot)$: Model parameter for GC EOS

$\Omega(\cdot)$: Model parameter for GC EOS

$\Omega_{\mu,i}(\cdot)$: Viscosity Collision integral of ith species

$\omega_i(\cdot)$: Acentric factor of ith species in GC EOS

Subscripts

c : Critical point (temperature, pressure, compressibility factor model parameter for GC EOS)

i, j : Species

k : Term of dimensionless parameter-independent function $\gamma(\cdot)$

r : Reduced variable (temperature, pressure)

Introduction

The calculation of pressure drops associated with gas transmission in pipelines has been the subject of several research and teaching efforts. Bird, Stewart, and Lightfoot in [BSL07, p. 464-465] presented a dimensional ODE model and its integral form under the ideal gas assumption, which they subsequently applied for pressure drop prediction to the pipeline transmission of pure methane. Cristello et. al. [Cri23] pursued development of a dimensional gas hydraulic model for simulation of a transmission/distribution pipeline, as well as application of the real-time transient model for leak detection in H₂ blended pipelines. They found that up to a 30% blend of H₂ can be transported without substantial changes to material or compressor station layout, or up to 60% H₂ with compressor upgrading. Zhang et. al. [Zha24] used the Benedict-Webb-Rubin (BWR) equation of state (EOS) in a dimensional model used for power optimization of a single pipeline and pipeline networks with multiple sources. Multi-objective optimization strategies were employed for the multi-source pipeline network. Abbas et. al. [Abb21] employed SRK, PR, Benedict-Webb-Rubin-Starling (BWRS) EOS for thermodynamic calculations. Their resulting dimensional model generated velocity profiles for which the erosional velocity limit of the pipeline was shown not be possible to reach for H₂ blends up to 40%. Li, et. al. [Li21] covered the impact of pipeline H₂ blending on the Joule-Thomson coefficient of NG, H₂ blending ratios from 5% to 30%, employing the SRK, PR, and BWRS EOS. A database of J-T coefficients for 5%-30% H₂ blending, 0.5-20MPa pressures, and temperatures of 275, 300, 350K was generated using a dimensional model. Experimental validation of the calculations showed BWRS EOS to be most accurate in identifying the J-T coefficient. Abd et. al. [Abd21] simulated a 94km pipeline (“Ruswil – Griespass string part of the Transitgas project”) on Aspen Hysys Version 9 using the Peng-Robinson EOS, assuming effects of compressor stations to be negligible. Notably, they found that viscosity of the mixture increases for up to 2% H₂ blend, then decreases as H₂ concentration further increases. Elevation effects were studied for changes of 25m uphill and downhill, and found that increase in elevation results in an increase in pressure drop. Dimensional modeling and experimental results from Bainier, et. al. [Bai19] and Allison, et. al. [All21] show that for 85% H₂ blends, the pipeline energy flowrate capacity reaches a minimum value and pressure drop achieves a maximum value. Our work first provides an analytical solution to a general, dimensionless, pressure drop prediction model, which only requires pipeline dimensionless inlet pressure and three temperature, geometry and flow related dimensionless parameter information to provide dimensionless and dimensional pressure drop estimates for general nonideal gas mixtures featuring various cubic EOS models, and then illustrates the model’s predictions for pure methane-hydrogen and eight species containing natural gas-hydrogen blends.

Thermodynamic and Transport Mixture Properties

Equation of State

The thermodynamic nature of the considered gas mixtures is captured by the Ideal Gas and Generic Cubic Equations Of State (IGEOS, GCEOS), [SVAS22, p. 77-78, p. 97-98, p. 503],

which determine the gas' pressure P as a function of temperature T and molar volume V as:

$$\text{IGEOS: } P : \mathbb{R}^+ \times (0, \infty) \rightarrow \mathbb{R}^+, \quad P : (T, V) \rightarrow P(T, V) \triangleq \frac{RT}{V} \quad (1)$$

$$\boxed{\begin{aligned} &P : D_P \rightarrow \mathbb{R}, \quad P : (T, V) \rightarrow P(T, V) \triangleq \frac{RT}{V - b} - \frac{a(T)}{(\sigma - \varepsilon)b} \left[\frac{1}{(V + \varepsilon b)} - \frac{1}{(V + \sigma b)} \right] \\ &D_P \triangleq \{(T, V) \in \mathbb{R}^+ \times (b, \infty) : V \notin \{\{-\varepsilon b\} \cup \{-\sigma b\}\} \cap \mathbb{R}^+\} \\ &\text{GCEOS: } b \triangleq \sum_{i=1}^N y_i b_i > 0, \quad b_i \triangleq \Omega \frac{RT_{c,i}}{P_{c,i}} > 0, \quad T_{r,i} \triangleq \frac{T}{T_{c,i}} > 0, \quad \sigma > \varepsilon \\ &a(T) \triangleq \sum_{i=1}^N \sum_{j=1}^N y_i y_j (a_i(T) a_j(T))^{1/2} > 0, \quad a_i(T) \triangleq \Psi \frac{\alpha(T_{r,i}; \omega_i) R^2 T_{c,i}^2}{P_{c,i}} > 0 \end{aligned}} \quad (2)$$

where $R(J/(mol \cdot K)) \triangleq k \cdot N_A = 8.314$, $k(J/K) \triangleq 1.380649 \cdot 10^{-23}$, $N_A(1/mol) \triangleq 6.02214076 \cdot 10^{23}$, and $P_{c,i}$, $T_{c,i}$, ω_i , y_i are the i th species' critical pressure, critical temperature, acentric factor, and mole fraction, and R, k, N_A are the Universal Gas Constant, Boltzmann constant, and Avogadro number, [SI19].

The aforementioned IGEOS, GCEOS can also be used to determine the gas' molar volume V as a function of temperature T and pressure P as:

$$\text{IGEOS: } V : \mathbb{R}^+ \times (0, \infty) \rightarrow \mathbb{R}^+, \quad V : (T, P) \rightarrow V(T, P) \triangleq \frac{RT}{P} \quad (3)$$

GCEOS:

$$\boxed{\begin{aligned} &V : \mathbb{R}^+ \times (0, \infty) \rightarrow \mathbb{R}^+, \quad V : (T, P) \rightarrow V(T, P) : V(T, P) \text{ is largest root of} \\ &V^3 + \left[(\varepsilon + \sigma - 1)b - \frac{RT}{P} \right] V^2 + \left[(\varepsilon\sigma - \varepsilon - \sigma)b^2 - \frac{RT}{P}(\varepsilon + \sigma)b + \frac{a(T)}{P} \right] V - \left[\varepsilon\sigma b^3 + \frac{RT}{P} \varepsilon\sigma b^2 + \frac{a(T)}{P} b \right] = 0 \\ &b \triangleq \Omega \sum_{i=1}^N \left(y_i \frac{RT_{c,i}}{P_{c,i}} \right), \quad a(T) \triangleq \Psi R^2 \sum_{i=1}^N \sum_{j=1}^N y_i y_j \left(\frac{\alpha\left(\frac{T}{T_{c,i}}; \omega_i\right) T_{c,i}^2}{P_{c,i}} - \frac{\alpha\left(\frac{T}{T_{c,j}}; \omega_j\right) T_{c,j}^2}{P_{c,j}} \right)^{1/2} \end{aligned}} \quad (4)$$

It is important to point out that the aforementioned IGEOS and GCEOS models do not yield necessarily equal molar volume V values for a gas mixture of a given composition (in mole fraction $\{y_i\}_{i=1}^N$ terms), temperature T , and pressure P , and do not yield necessarily equal pressure P values for a gas mixture of a given composition (in mole fraction $\{y_i\}_{i=1}^N$ terms), temperature T , and molar volume V .

The considered GCEOS models are listed in Table 1 below:

Table 1: GCEOS Parameters

E.O.S.	$\alpha(T_{r,i}; \omega_i)$	σ	ε	Ω	Ψ	Z_c
$RK(1949)$	$(T_{r,i})^{\frac{-1}{2}}$	1	0	0.08664	0.42748	$1/3$
$SRK(1972)$	$\left[1 + \begin{pmatrix} 0.480 + \\ + 1.574\omega_i - 0.176\omega_i^2 \end{pmatrix} \left(1 - (T_{r,i})^{\frac{1}{2}}\right)\right]^2$	1	0	0.08664	0.42748	$1/3$
$PR(1976)$	$\left[1 + \begin{pmatrix} 0.37464 + \\ + 1.54226\omega_i - 0.26992\omega_i^2 \end{pmatrix} \left(1 - (T_{r,i})^{\frac{1}{2}}\right)\right]^2$	$1 + \sqrt{2}$	$1 - \sqrt{2}$	0.07780	0.45724	0.30740

The gas mixture's mass density is directly related to the gas mixture's molar mass, and molar volume, which satisfy the following relations:

$$\boxed{\rho = \frac{M}{V}, M = \sum_{i=1}^N M_i y_i, M_i = m_i \cdot N_A, i = 1, N} \quad (5)$$

where ρ, M, V are the mixture's mass density, molar mass and molar volume, and M_i, y_i, m_i are the i th species' molar mass, molar fraction, and single molecule's mass.

Introducing the following variables, then yields the dimensionless IGEOS and GCEOS (DIGEOS, DGCEOS) listed below.

$$\boxed{\beta \triangleq \frac{Pb}{RT}, q \triangleq \frac{a(T)}{bRT}, \tilde{V} \triangleq \frac{V}{b}} \quad (6)$$

$$b_i^{IG} \triangleq \frac{RT_{c,i}}{P_{c,i}} = \frac{b_i}{\Omega}, b^{IG} \triangleq \sum_{i=1}^N y_i b_i^{IG} = \frac{b}{\Omega}, \beta^{IG} \triangleq \frac{Pb^{IG}}{RT} = \frac{\beta}{\Omega}, \tilde{V}^{IG} \triangleq \frac{V}{b^{IG}} = \frac{\Omega V}{b} = \Omega \tilde{V}$$

$$\text{DIGEOS: } \boxed{\beta^{IG} : (0, \infty) \rightarrow \mathbb{R}^+, \beta^{IG} : \tilde{V}^{IG} \rightarrow \beta^{IG}(\tilde{V}^{IG}) \triangleq \frac{1}{\tilde{V}^{IG}}} \quad (7)$$

$$\boxed{\beta : D_\beta \rightarrow \mathbb{R}^+, \beta : (q, \tilde{V}) \rightarrow \beta(q, \tilde{V}) \triangleq \frac{1}{\tilde{V}-1} - \frac{q}{\sigma-\varepsilon} \left[\frac{1}{(\tilde{V}+\varepsilon)} - \frac{1}{(\tilde{V}+\sigma)} \right]} \quad (8)$$

$$\text{DGCEOS: } D_\beta \triangleq \left\{ (q, \tilde{V}) \in \mathbb{R}^+ \times (1, \infty) : \tilde{V} \notin \left\{ \{ -\varepsilon \} \cup \{ -\sigma \} \right\} \cap \mathbb{R}^+ \right\}$$

$$q \triangleq \frac{a(T)}{bRT} = \frac{\sum_{i=1}^N \sum_{j=1}^N y_i y_j (a_i(T) a_j(T))^{1/2}}{RT \sum_{i=1}^N y_i b_i}, \left\{ \begin{array}{l} b_i \triangleq \Omega \frac{RT_{c,i}}{P_{c,i}} > 0, T_{r,i} \triangleq \frac{T}{T_{c,i}} > 0, \sigma > \varepsilon \\ a_i(T) \triangleq \Psi \frac{\alpha(T_{r,i}; \omega_i) R^2 T_{c,i}^{-2}}{P_{c,i}} > 0 \end{array} \right\}$$

The above DGCEOS establishes the dimensionless nonideal gas mixture pressure $\beta \triangleq \frac{Pb}{RT}$,

normalized by temperature, and the GCEOS parameter b accounting for finite molecule size, as a function of the dimensionless nonideal gas mixture's temperature q and dimensionless molar volume \tilde{V} , i.e., $\beta(q, \tilde{V})$, which in turn implies that:

$$d\beta = \frac{\partial \beta(q, \tilde{V})}{\partial q} dq + \frac{\partial \beta(q, \tilde{V})}{\partial \tilde{V}} d\tilde{V}, \text{ where}$$

$$\left\{ \begin{array}{l} \frac{\partial \beta(q, \tilde{V})}{\partial q} = \frac{-1}{\sigma - \varepsilon} \left[\frac{1}{(\tilde{V} + \varepsilon)} - \frac{1}{(\tilde{V} + \sigma)} \right] \\ \frac{\partial \beta(q, \tilde{V})}{\partial \tilde{V}} = \frac{-1}{(\tilde{V} - 1)^2} + \frac{q}{\sigma - \varepsilon} \left[\frac{1}{(\tilde{V} + \varepsilon)^2} - \frac{1}{(\tilde{V} + \sigma)^2} \right] \end{array} \right\}, \sigma > \varepsilon$$

The aforementioned DIGEOS, DGCEOS can also be used to determine the gas' dimensionless molar volume \tilde{V} as a function of dimensionless temperature q , and dimensionless pressure β as:

$$\text{DIGEOS: } \tilde{V}^{IG} : (0, \infty) \rightarrow \mathbb{R}^+, \tilde{V}^{IG} : \beta^{IG} \rightarrow \tilde{V}^{IG} (\beta^{IG}) = \frac{1}{\beta^{IG}} = \frac{1}{\frac{P}{T} \sum_{i=1}^N \left(y_i \frac{T_{c,i}}{P_{c,i}} \right)} \quad (9)$$

DGGCEOS:

$$\boxed{\begin{aligned} & \tilde{V} : \mathbb{R}^+ \times (0, \infty) \rightarrow \mathbb{R}^+, \tilde{V} : (q, \beta) \rightarrow \tilde{V}(q, \beta) : \tilde{V}(q, \beta) \text{ is largest root of} \\ & \tilde{V}^3 + \tilde{V}^2 \left(-\frac{1}{\beta} - 1 + \sigma + \varepsilon \right) + \tilde{V} \left(-\varepsilon - \sigma + \sigma\varepsilon - \frac{(\sigma + \varepsilon - q)}{\beta} \right) + \left(-\sigma\varepsilon - \frac{\sigma\varepsilon + q}{\beta} \right) = 0 \\ & \Psi \sum_{i=1}^N \sum_{j=1}^N y_i y_j \left(\frac{\alpha \left(\frac{T}{T_{c,i}}; \omega_i \right) T_{c,i}^2}{P_{c,i}} \frac{\alpha \left(\frac{T}{T_{c,j}}; \omega_j \right) T_{c,j}^2}{P_{c,j}} \right)^{1/2} \\ & \beta \triangleq \frac{Pb}{RT} = \Omega \sum_{i=1}^N \left(y_i \frac{P}{P_{c,i}} \frac{T_{c,i}}{T} \right), q \triangleq \frac{a(T)}{bRT} = \frac{\Omega T \sum_{i=1}^N \left(y_i \frac{T_{c,i}}{P_{c,i}} \right)}{\Omega T \sum_{i=1}^N \left(y_i \frac{T_{c,i}}{P_{c,i}} \right)} \end{aligned}} \quad (10)$$

Further, it is also important to point out that the aforementioned DIGEOS and DGCEOS models also do not necessarily yield the same dimensionless molar volume \tilde{V} for a gas mixture of a given composition (in mole fraction $\{y_i\}_{i=1}^N$ terms) temperature T and pressure P . However, given the above definitions of β^{IG} , \tilde{V}^{IG} , b^{IG} , β , \tilde{V} , b , it holds that for a gas mixture of a given composition (in mole fraction $\{y_i\}_{i=1}^N$ terms) temperature T and pressure P , it holds:

$$\boxed{\beta^{IG} \triangleq \frac{Pb^{IG}}{RT} = \sum_{i=1}^N \left(y_i \frac{P}{P_{c,i}} \frac{T_{c,i}}{T} \right), \beta \triangleq \frac{Pb}{RT} = \Omega \sum_{i=1}^N \left(y_i \frac{P}{P_{c,i}} \frac{T_{c,i}}{T} \right) = \Omega \frac{Pb^{IG}}{RT} = \Omega \beta^{IG}} \quad (11)$$

while for a gas mixture of a given composition (in mole fraction $\{y_i\}_{i=1}^N$ terms) and molar volume V it holds:

$$\boxed{\tilde{V}^{IG} \triangleq \frac{V}{b^{IG}} = \frac{V}{\sum_{i=1}^N \left(y_i \frac{RT_{c,i}}{P_{c,i}} \right)}, \quad \tilde{V} \triangleq \frac{V}{b} = \frac{V}{\Omega \sum_{i=1}^N \left(y_i \frac{RT_{c,i}}{P_{c,i}} \right)} = \frac{\tilde{V}^{IG}}{\Omega}} \quad (12)$$

It should also be pointed out that, for a given $\beta^{IG} \triangleq \frac{Pb^{IG}}{RT} = \sum_{i=1}^N \left(y_i \frac{P}{P_{c,i}} \frac{T_{c,i}}{T} \right)$, the DIGEOS model

enables the immediate evaluation of $\tilde{V}^{IG}(\beta^{IG}) = \frac{1}{\beta^{IG}}$, while the DGCEOS model for the evaluation of $\tilde{V}(q, \beta)$ through solution of the cubic eqn. (10), requires first the evaluation of

$$\beta = \Omega \beta^{IG} = \Omega \frac{Pb^{IG}}{RT} = \Omega \sum_{i=1}^N \left(y_i \frac{P}{P_{c,i}} \frac{T_{c,i}}{T} \right) \text{ and the evaluation of}$$

$$\Psi \sum_{i=1}^N \sum_{j=1}^N y_i y_j \left(\frac{\alpha \left(\frac{T}{T_{c,i}}; \omega_i \right) T_{c,i}^2}{P_{c,i}} - \frac{\alpha \left(\frac{T}{T_{c,j}}; \omega_j \right) T_{c,j}^2}{P_{c,j}} \right)^{1/2}$$

$$q \triangleq \frac{a(T)}{bRT} = \frac{1}{\Omega T \sum_{i=1}^N \left(y_i \frac{T_{c,i}}{P_{c,i}} \right)}.$$

To facilitate the comparison of molar volume V IGEOS and GCEOS predictions for a gas mixture of a given composition (in mole fraction $\{y_i\}_{i=1}^N$ terms), temperature T , and pressure P , when dimensionless DIGEOS and DGCEOS computations are carried out, the Figures 1, 2 shown below are created, in which the DIGEOS \tilde{V}^{IG} , β^{IG} values are plotted against the bottom and left axes, while the DGCEOS \tilde{V} , β values are plotted against the top and right axes, which relate to each other based on the equations $\tilde{V}^{IG} = \Omega \tilde{V}$ and $\beta^{IG} = \frac{\beta}{\Omega}$.

Based on the $\{y_i\}_{i=1}^N$, T , P information and the DGCEOS model choice, β , β^{IG} , q are first calculated. The value of the latter quantity, q , identifies the relevant dimensionless DGCEOS iso- q curve, while the β , β^{IG} values lie at the same horizontal line since

$\beta = \Omega \sum_{i=1}^N \left(y_i \frac{P}{P_{c,i}} \frac{T_{c,i}}{T} \right) = \Omega \beta^{IG}$. Then, \tilde{V} , \tilde{V}^{IG} are identified as the projections of the intersections

of the aforementioned horizontal line with the aforementioned DGCEOS iso- q curve and the

DIGEOS curve on the top and bottom axes respectively. Then, since $\tilde{V}^{IG} \triangleq \frac{V}{b^{IG}} = \frac{\Omega V}{b} = \Omega \tilde{V}$, if

these projections are on the same vertical line, then the IGEOS and GCEOS molar volume predictions would be equal.

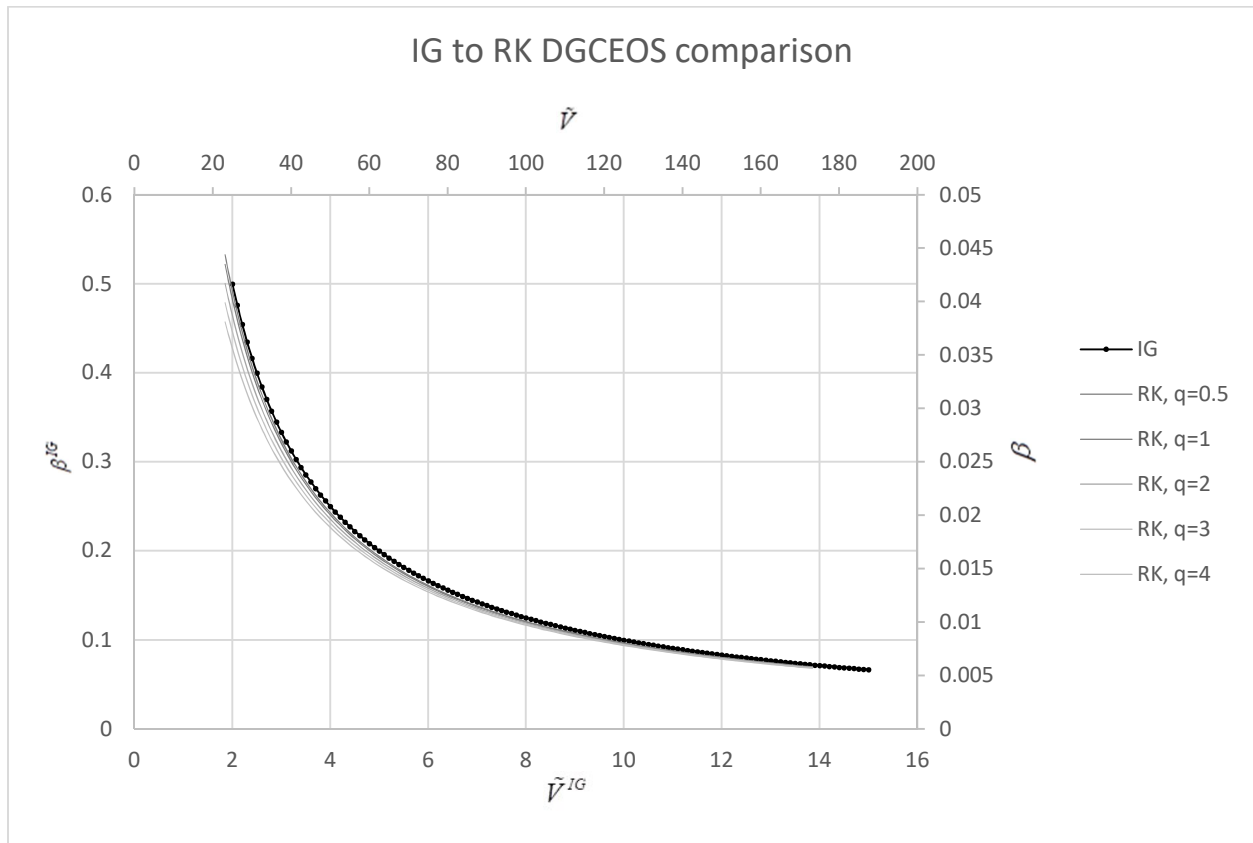


Figure 1: DIGEOS \tilde{V}^{IG} , β^{IG} , Redlich/Kwong, Soave/Redlich/Kwong DGCEOS \tilde{V} , β iso- q curves

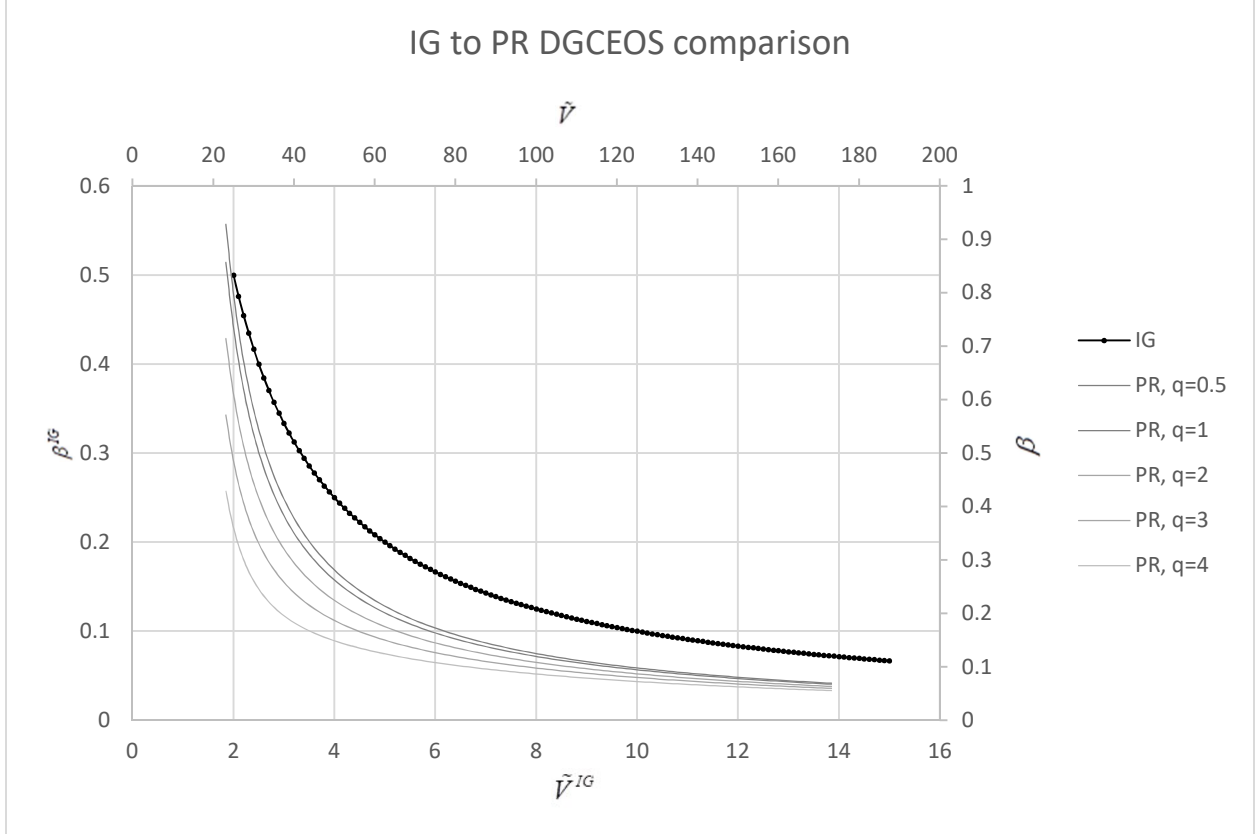


Figure 2: DIGEOS \tilde{V}^{IG} , β^{IG} , Peng/Robinson DGCEOS \tilde{V} , β iso- q curves

Viscosity

The considered nonideal gas mixture is a Newtonian fluid, whose viscosity is considered to be a function of temperature, $\mu(T)$, and is identified by the semiempirical formulas shown below, whose mixing rules were first developed by Wilke [Wil50], modified in [BSL02], and listed in eqns. 1.4-15, 1.4-16, [BSL07, p. 27], and eqns. 12.117, 12.118, [KCG03, p. 518-519], whose species' viscosities $\mu_i(T)$, $i = 1, N$ (also considered to be only functions of temperature) are described by a kinetic theory derived expression listed in eqn. 1.4-14, [BSL07, p. 26], and eqn. 12.100, [KCG03, p. 516], and whose species' viscosity collision integrals $\Omega_{\mu,i}(T)$, $i = 1, N$ are expressed using a curve-fitted expression developed by [NJA72], presented in eqn. E.2-1, [BSL07, p. 866].

$$\begin{aligned}
\mu(T) &= \sum_{i=1}^N \frac{y_i \mu_i(T)}{\sum_{j=1}^N y_j \Phi_{i,j}(T)}, \quad \Phi_{i,j}(T) = \frac{\left[1 + (\mu_i(T)/\mu_j(T))^{1/2} \cdot (M_j/M_i)^{1/4}\right]^2}{\left[8(1 + (M_i/M_j))\right]^{1/2}}, \quad i=1, N; j=1, N \\
\mu_i(T) &= \frac{5}{16\sqrt{\pi}} \frac{\sqrt{m_i k T}}{\sigma_i^2 \Omega_{\mu,i}(T)} = \frac{5}{16\sqrt{\pi}} \frac{\sqrt{M_i R T}}{N \sigma_i^2 \Omega_{\mu,i}(T)} \\
\Omega_{\mu,i}(T) &= \frac{1.16145}{(T_i^*)^{0.14874}} + \frac{0.52487}{\exp(0.77320 \cdot T_i^*)} + \frac{2.16178}{\exp(2.43787 \cdot T_i^*)}, \quad T_i^* \triangleq \frac{k T}{\epsilon_i}
\end{aligned} \tag{13}$$

where $M_i, y_i, m_i, \sigma_i, T_i^*, \epsilon_i$ are the ith species' molar mass, mole fraction, single molecule's mass, collision diameter of its Lennard Jones potential, dimensionless temperature, and its Lennard Jones potential related parameter denoting the maximum energy of attraction between two molecules of the ith species, and k is the Boltzmann constant. The Lennard Jones potential related parameters $\sigma_i \left(\text{Å} \right), \frac{\epsilon_i}{k} (K)$ for various species are provided in Table E.1 of [BSL07, p. 864-865].

Pipeline model

This study focuses on the steady state, isothermal flow of a nonideal, compressible, gas mixture flowing through a straight cylindrical pipeline of constant diameter D_p , which implies that the pipeline has a constant hydraulic radius R_h , and a constant cross section A_p , length L_p , and differential length dl .

Then, using eqn. 6.2-16, [BSL07, p. 183], yields the following relations among the aforementioned pipeline parameters:

$$R_h = \frac{D_p}{4} > 0, \quad A_p = \pi \frac{D_p^2}{4} = 4\pi R_h^2 > 0.$$

Friction factor model

The gas mixture's friction factor f can be expressed in terms of the fluid flow's Reynolds number Re defined by eqn. 6.2-18 in [BSL07, p. 183], using the empirical relations by Haaland eqn. 6.2-15 in [BSL07, p. 182], or eqn. 6.21 in [DeN05, p.187]

$$\begin{aligned}
\frac{1}{\sqrt{f}} &= -3.6 \cdot \log_{10} \left[\frac{6.9}{Re} + \left(\frac{(\kappa/D_p)}{3.7} \right)^{10} \right] \text{ if } \left\{ \begin{array}{l} 4 \cdot 10^4 < Re < 10^8 \\ 0 < \kappa/D_p < 0.05 \end{array} \right\} \\
f &= 0.001375 \cdot \left[1 + \left(20,000 \left(\kappa/D_p \right) + \frac{10^6}{Re} \right)^{\frac{1}{3}} \right] \\
Re &= \frac{D_p v \rho}{\mu(T)} = \frac{4 \dot{m}}{\pi \cdot D_p \cdot \mu(T)}
\end{aligned} \tag{14}$$

where κ is a constant that defines pipeline roughness to be used in friction factor relations.

Mechanical Energy Balance Model

Considering that the flow is isothermal, the gas mixture's mechanical energy balance over a pipeline section with no differential height, differential length dl yields the following equation, based on eqn. 15.4-2, [BSL07, p. 461]:

$$vdv + \frac{1}{\rho} dP = d\hat{W} - \frac{1}{2} v^2 \frac{f}{R_h} dl$$

where v is the gas mixture's velocity, $d\hat{W}$ is the differential amount of work per unit mass possibly provided to the gas mixture, and f is the friction factor of the nonideal gas mixture.

Considering no compression equipment exists within the pipeline section yields $d\hat{W} = 0$, and incorporating the aforementioned pipeline geometric relations results in the relation:

$$\rho v dv + dP + \rho \frac{2v^2 f}{D_p} dl = 0.$$

Considering that the gas flow is steady-state, implies that \dot{m} is constant. Given that the cylindrical pipeline has a constant cross-sectional area A_p , and denoting ρ_0, v_0, V_0 to be the gas mixture's mass density, velocity and molar volume at the pipeline inlet respectively, then

$$\text{implies: } \left\{ \begin{array}{l} \dot{m} = \rho \cdot v \cdot A_p = \frac{M}{V} \cdot v \cdot A_p = \frac{M}{V} \cdot v \cdot \frac{\pi \cdot D_p^2}{4} \\ \dot{m} = \rho_0 \cdot v_0 \cdot A_p = \frac{M}{V_0} \cdot v_0 \cdot A_p = \frac{M}{V_0} \cdot v_0 \cdot \frac{\pi \cdot D_p^2}{4} \end{array} \right\} \Rightarrow \frac{v}{V} = \frac{v_0}{V_0} = \frac{4\dot{m}}{M \cdot \pi \cdot D_p^2}.$$

Then the differential form of the mechanical energy balance becomes:

$$\begin{aligned} & \frac{M}{V} \left(\frac{4\dot{m}}{M \cdot \pi \cdot D_p^2} \right) V d \left(\frac{4\dot{m}}{M \cdot \pi \cdot D_p^2} V \right) + \frac{M}{V} \left(\frac{2f}{D_p} \left(\frac{4\dot{m}}{M \cdot \pi \cdot D_p^2} \right)^2 V^2 \right) dl + dP = 0 \xrightarrow[\dot{m}=\text{constant}]{\{y_i\}_{i=1}^N=\text{constant}} \\ & M \left(\frac{4\dot{m}}{M \cdot \pi \cdot D_p^2} \right)^2 dV + M \left(\frac{2f}{D_p} \left(\frac{4\dot{m}}{M \cdot \pi \cdot D_p^2} \right)^2 V \right) dl + dP = 0 \end{aligned}$$

Introducing the additional dimensionless variables listed below, allows the expression of the above relation in dimensionless form utilizing the IGEOS, GCEOS, and DIGEOS, DGCEOS.

$$\begin{aligned}
& \tilde{l} \triangleq \frac{l}{L_p} \in (0,1), \tilde{v} \triangleq \frac{v}{v_0} > 0, \tilde{V}_0^{IG} \triangleq \frac{V_0}{b^{IG}} = \frac{v_0 \cdot M \cdot \pi \cdot D_p^2}{4\dot{m}b^{IG}} \\
& \tilde{V}_0 \triangleq \frac{V_0}{b} = \frac{v_0 \cdot M \cdot \pi \cdot D_p^2}{4\dot{m}b} = \frac{v_0 \cdot M \cdot \pi \cdot D_p^2}{4\dot{m}\Omega b^{IG}} = \frac{\tilde{V}_0^{IG}}{\Omega} \\
& r_{LD} \triangleq \frac{D_p}{L_p} \in (0,1), r_{KI}^{IG} \triangleq \frac{M}{RT} \left(\frac{4\dot{m}b^{IG}}{M \cdot \pi \cdot D_p^2} \right)^2 = \frac{M}{RT} \left(\frac{v_0}{\tilde{V}_0^{IG}} \right)^2 \\
& r_{KI} \triangleq \frac{M}{RT} \left(\frac{4\dot{m}b}{M \cdot \pi \cdot D_p^2} \right)^2 = \frac{M}{RT} \left(\frac{v_0}{\tilde{V}_0} \right)^2 = \frac{\Omega^2 M}{RT} \left(\frac{v_0}{\tilde{V}_0^{IG}} \right)^2 = \Omega^2 r_{KI}^{IG}
\end{aligned} \tag{15}$$

The Theorem below provides the dimensionless expressions of the integrated form of the mechanical energy balance. Its proof is provided in Appendix A.1.

Theorem

The integrated dimensionless forms of the mechanical energy balance (DIGMEB, DGCMEB) for the isothermal, steady-state flow of a gas mixture over a horizontal, cylindrical pipeline are:

a. DIGMEB for DIGEOS:

$$\begin{aligned}
& \gamma^{IG}(\tilde{V}^{IG}(1)) - \gamma^{IG}(\tilde{V}_0^{IG}) = \frac{2f}{r_{LD}}, \gamma^{IG}(\tilde{V}^{IG}) \triangleq \gamma_1(\tilde{V}^{IG}) + \frac{1}{r_{KI}^{IG}} \cdot \gamma_2^{IG}(\tilde{V}^{IG}) \quad \forall \tilde{V}^{IG} \\
& \left\{ \gamma_1(\tilde{V}^{IG}) \triangleq -\ln(\tilde{V}^{IG}), \gamma_2^{IG}(\tilde{V}^{IG}) \triangleq \frac{-1}{2(\tilde{V}^{IG})^2}, \gamma^{IG}(\tilde{V}^{IG}) \triangleq \gamma_1(\tilde{V}^{IG}) + \frac{1}{r_{KI}^{IG}} \gamma_2^{IG}(\tilde{V}^{IG}) \right\} \quad \forall \tilde{V}^{IG}
\end{aligned} \tag{16}$$

b. DGCMEB for GCEOS:

$$\boxed{
\begin{aligned}
\gamma^{\varepsilon\sigma}(\tilde{V}(1)) - \gamma^{\varepsilon\sigma}(\tilde{V}_0) &= \frac{2f}{r_{LD}} \text{if } \begin{cases} \varepsilon \neq 0 \\ \sigma \neq 0 \end{cases} \\
\gamma^{0\sigma}(\tilde{V}(1)) - \gamma^{0\sigma}(\tilde{V}_0) &= \frac{2f}{r_{LD}} \text{if } \begin{cases} \varepsilon = 0 \\ \sigma \neq 0 \end{cases} \\
\gamma^{\varepsilon\sigma}(\tilde{V}) &\triangleq \left[\gamma_1(\tilde{V}) + \frac{1}{r_{KI}} \cdot \gamma_2^{GC}(\tilde{V}) + \frac{q}{r_{KI}} \cdot \gamma_3^{\varepsilon\sigma}(\tilde{V}) \right] \forall \tilde{V} \text{ if } \begin{cases} \varepsilon \neq 0 \\ \sigma \neq 0 \end{cases} \\
\gamma^{0\sigma}(\tilde{V}) &\triangleq \left[\gamma_1(\tilde{V}) + \frac{1}{r_{KI}} \cdot \gamma_2^{GC}(\tilde{V}) + \frac{q}{r_{KI}} \cdot \gamma_3^{0\sigma}(\tilde{V}) \right] \forall \tilde{V} \text{ if } \begin{cases} \varepsilon = 0 \\ \sigma \neq 0 \end{cases} \\
\gamma_1(\tilde{V}) &\triangleq -\ln(\tilde{V}) \quad \forall \tilde{V}, \quad \gamma_2^{GC}(\tilde{V}) \triangleq \ln\left(\frac{\tilde{V}}{\tilde{V}-1}\right) - \frac{1}{(\tilde{V}-1)} \quad \forall \tilde{V}, \\
\gamma_3^{\varepsilon\sigma}(\tilde{V}) &\triangleq \frac{-1}{\varepsilon^2(\sigma-\varepsilon)} \left[\ln\left(\frac{\tilde{V}}{\varepsilon+\tilde{V}}\right) + \frac{\varepsilon}{\varepsilon+\tilde{V}} \right] + \frac{1}{\sigma^2(\sigma-\varepsilon)} \left[\ln\left(\frac{\tilde{V}}{\sigma+\tilde{V}}\right) + \frac{\sigma}{\sigma+\tilde{V}} \right] \quad \forall \tilde{V} \text{ if } \begin{cases} \varepsilon \neq 0 \\ \sigma \neq 0 \end{cases} \\
\gamma_3^{0\sigma}(\tilde{V}) &\triangleq \frac{1}{\sigma^2} \left[\frac{1}{\sigma} \ln\left(\frac{\tilde{V}}{\sigma+\tilde{V}}\right) + \frac{1}{\sigma+\tilde{V}} \right] + \frac{1}{2\sigma(\tilde{V})^2} \quad \forall \tilde{V} \text{ if } \begin{cases} \varepsilon = 0 \\ \sigma \neq 0 \end{cases}
\end{aligned} \tag{17}
}$$

The Theorem's application to the considered DIGEOS, DGCEOS models yields the table below:

Table 2: γ^{IG} , $\gamma^{0\sigma}$, $\gamma^{\varepsilon\sigma}$ functions involved in DIGMEB, DGCMEB models

<i>Ideal Gas</i>	$\gamma^{IG}(\tilde{V}^{IG}) \triangleq \left[\gamma_1(\tilde{V}^{IG}) + \frac{1}{r_{K1}} \gamma_2^{IG}(\tilde{V}^{IG}) \right] = \left[-\ln(\tilde{V}^{IG}) + \frac{1}{r_{K1}} \left(\frac{-1}{2(\tilde{V}^{IG})^2} \right) \right]$
<i>RK(1949)</i>	$\gamma^{0\sigma}(\tilde{V}) \triangleq \begin{bmatrix} \gamma_1(\tilde{V}) + \\ + \frac{1}{r_{K1}} \cdot \gamma_2^{0\sigma}(\tilde{V}) + \\ + \frac{q}{r_{K1}} \cdot \gamma_3^{0\sigma}(\tilde{V}) \end{bmatrix} = \left[-\ln(\tilde{V}) + \frac{1}{r_{K1}} \cdot \begin{bmatrix} \ln\left(\frac{\tilde{V}}{\tilde{V}-1}\right) - \\ \frac{1}{(\tilde{V}-1)} \end{bmatrix} + \frac{q}{r_{K1}} \cdot \begin{bmatrix} \ln\left(\frac{\tilde{V}}{\tilde{V}+1}\right) + \frac{1}{\tilde{V}+1} + \frac{1}{2(\tilde{V})^2} \end{bmatrix} \right]$
<i>SRK(1972)</i>	$\gamma^{0\sigma}(\tilde{V}) \triangleq \begin{bmatrix} \gamma_1(\tilde{V}) + \\ + \frac{1}{r_{K1}} \cdot \gamma_2^{0\sigma}(\tilde{V}) + \\ + \frac{q}{r_{K1}} \cdot \gamma_3^{0\sigma}(\tilde{V}) \end{bmatrix} = \left[-\ln(\tilde{V}) + \frac{1}{r_{K1}} \cdot \begin{bmatrix} \ln\left(\frac{\tilde{V}}{\tilde{V}-1}\right) - \\ \frac{1}{(\tilde{V}-1)} \end{bmatrix} + \frac{q}{r_{K1}} \cdot \begin{bmatrix} \ln\left(\frac{\tilde{V}}{\tilde{V}+1}\right) + \frac{1}{\tilde{V}+1} + \frac{1}{2(\tilde{V})^2} \end{bmatrix} \right]$
<i>PR(1976)</i>	$\gamma^{\varepsilon\sigma}(\tilde{V}) \triangleq \begin{bmatrix} \gamma_1(\tilde{V}) + \\ + \frac{1}{r_{K1}} \cdot \gamma_2^{\varepsilon\sigma}(\tilde{V}) + \\ + \frac{q}{r_{K1}} \cdot \gamma_3^{\varepsilon\sigma}(\tilde{V}) \end{bmatrix} = -\ln(\tilde{V}) + \frac{1}{r_{K1}} \cdot \begin{bmatrix} \ln\left(\frac{\tilde{V}}{\tilde{V}-1}\right) - \\ \frac{1}{(\tilde{V}-1)} \end{bmatrix} + \frac{q}{r_{K1}} \cdot \begin{bmatrix} \frac{-1}{(3-2\sqrt{2}) \cdot 2\sqrt{2}} \left[\ln\left(\frac{\tilde{V}}{1-\sqrt{2}+\tilde{V}}\right) + \frac{1-\sqrt{2}}{1-\sqrt{2}+\tilde{V}} \right] \\ + \frac{1}{(3+2\sqrt{2}) \cdot 2\sqrt{2}} \left[\ln\left(\frac{\tilde{V}}{1+\sqrt{2}+\tilde{V}}\right) + \frac{1+\sqrt{2}}{1+\sqrt{2}+\tilde{V}} \right] \end{bmatrix}$

In advance of the case study computations, it is important to assess the behavior of the $\gamma^{IG}(\tilde{V}^{IG})$ function involved in the DIGMEB for DIGEOS. The following holds:

$$\gamma^{IG}(\tilde{V}^{IG}) \triangleq \gamma_1(\tilde{V}^{IG}) + \frac{1}{r_{KI}^{IG}} \gamma_2^{IG}(\tilde{V}^{IG}) = -\ln(\tilde{V}^{IG}) - \frac{1}{2r_{KI}^{IG}(\tilde{V}^{IG})^2} \Rightarrow$$

$$\frac{d\gamma^{IG}(\tilde{V}^{IG})}{d\tilde{V}^{IG}} = -\frac{1}{\tilde{V}^{IG}} + \frac{1}{r_{KI}^{IG}(\tilde{V}^{IG})^3} \Rightarrow \frac{d\gamma^{IG}(\tilde{V}^{IG})}{d\tilde{V}^{IG}} \begin{cases} > 0 \quad \forall \tilde{V}^{IG} \in \left(0, \frac{1}{\sqrt{r_{KI}^{IG}}}\right) \\ = 0 \quad \forall \tilde{V}^{IG} = \frac{1}{\sqrt{r_{KI}^{IG}}} \\ < 0 \quad \forall \tilde{V}^{IG} \in \left(\frac{1}{\sqrt{r_{KI}^{IG}}}, +\infty\right) \end{cases}.$$

This implies that the $\gamma^{IG}(\tilde{V}^{IG})$ function is strictly monotonically increasing over $\left(0, \frac{1}{\sqrt{r_{KI}^{IG}}}\right)$,

strictly monotonically decreasing over $\left(\frac{1}{\sqrt{r_{KI}^{IG}}}, +\infty\right)$, and has a maximum at $\tilde{V}^{IG} = \frac{1}{\sqrt{r_{KI}^{IG}}}$ whose

value is: $\max_{\tilde{V}^{IG} \in (0, +\infty)} \gamma^{IG}(\tilde{V}^{IG}) = \gamma^{IG}\left(\frac{1}{\sqrt{r_{KI}^{IG}}}\right) = \frac{1}{2}(\ln(r_{KI}^{IG}) - 1) \begin{cases} > 0 \text{ if } r_{KI}^{IG} \in (e, +\infty) \\ = 0 \text{ if } r_{KI}^{IG} = e \\ < 0 \text{ if } r_{KI}^{IG} \in (0, e) \end{cases}.$

Further, $\lim_{\tilde{V}^{IG} \rightarrow +\infty} \gamma^{IG}(\tilde{V}^{IG}) = -\infty$, $\lim_{\tilde{V} \rightarrow +\infty} \gamma^{0\sigma}(\tilde{V}) = -\infty$, [Wol24c].

Given that the DIGMEB for DIGEOS has the form $\gamma^{IG}(\tilde{V}^{IG}(1)) - \gamma^{IG}(\tilde{V}_0^{IG}) = \frac{2f}{r_{LD}} = \frac{2fL_p}{D_p} > 0$, it

is clear that it must hold that $\gamma^{IG}(\tilde{V}^{IG}(1)) > \gamma^{IG}(\tilde{V}_0^{IG})$. At any intermediate pipeline length

$l < L_p$, DIGMEB for DIGEOS has the form $\gamma^{IG}\left(\tilde{V}^{IG}\left(\frac{l}{L_p}\right)\right) - \gamma^{IG}(\tilde{V}_0^{IG}) = \frac{2fl}{D_p} > 0$, which means

$\gamma^{IG}\left(\tilde{V}^{IG}\left(\frac{l}{L_p}\right)\right)$ is a linearly increasing function of l . Further, since the pipeline pressure (and

the dimensionless pipeline pressure β^{IG}) must be decreasing throughout the pipeline, and it

holds that $\beta^{IG}\left(\tilde{V}^{IG}\left(\frac{l}{L_p}\right)\right) = \frac{1}{\tilde{V}^{IG}\left(\frac{l}{L_p}\right)}$, it must then hold that $\tilde{V}^{IG}\left(\frac{l}{L_p}\right)$ is a strictly

monotonically increasing function of l . It therefore holds,

$\gamma^{IG} \left(\tilde{V}^{IG} \left(\frac{l_2}{L_p} \right) \right) > \gamma^{IG} \left(\tilde{V}^{IG} \left(\frac{l_1}{L_p} \right) \right) \Leftrightarrow l_2 > l_1 \Leftrightarrow \tilde{V}^{IG} \left(\frac{l_2}{L_p} \right) > \tilde{V}^{IG} \left(\frac{l_1}{L_p} \right)$, which in turn implies that

the $\gamma^{IG}(\tilde{V}^{IG})$ has to be a strictly monotonically increasing function of $\tilde{V}^{IG} = \frac{1}{\sqrt{r_{KI}^{IG}}}$ which based on

the earlier monotonicity analysis implies that the DIGMEB computations are physically

meaningful when $\tilde{V}^{IG}(1) \in \left(0, \frac{1}{\sqrt{r_{KI}^{IG}}} \right)$. The behavior of the $\gamma^{IG}(\tilde{V}^{IG})$, $\gamma^{0\sigma}(\tilde{V})$, $\gamma^{\varepsilon\sigma}(\tilde{V})$ functions

involved in the DIGMEB for DIGEOS, and DGCMEB for RK/SRK and PR GCEOS, within domains in which they are monotonically increasing is illustrated below in the Figures 3, 4, 5 for various iso- r_{KI}^{IG} , iso- (q, r_{KI}) , iso- (q, r_{KI}) curves respectively.

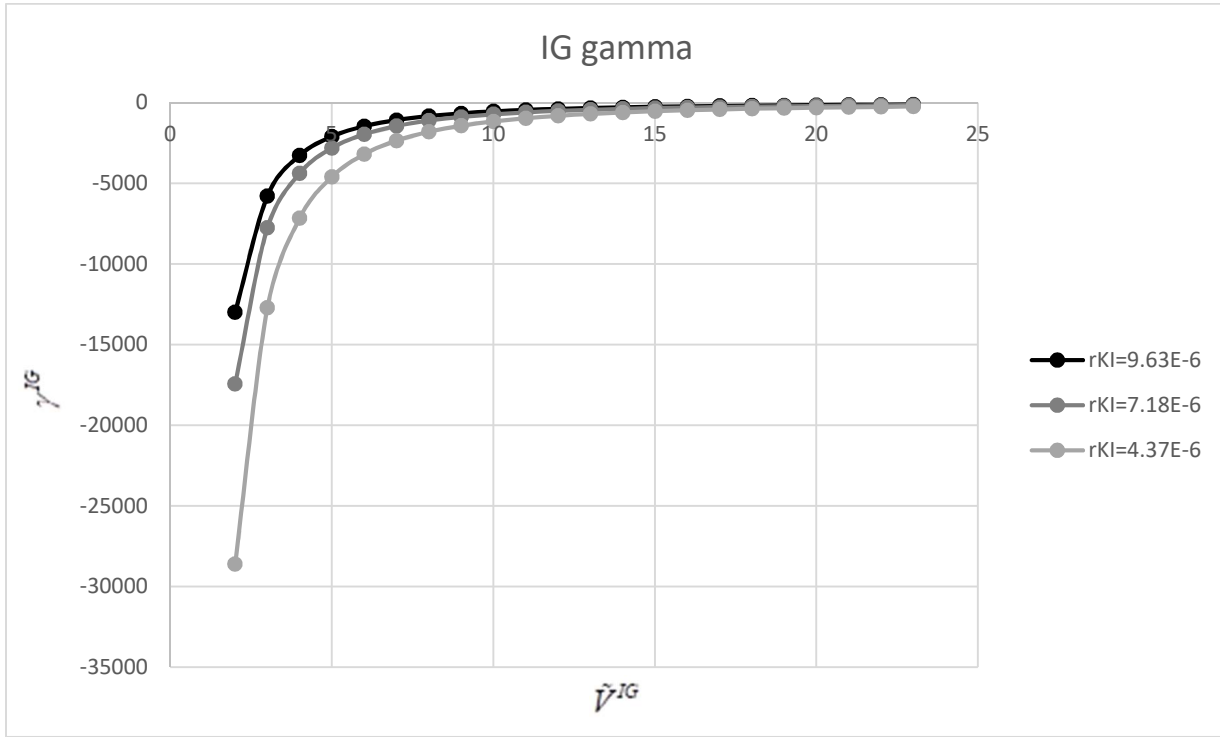


Figure 3: DIGEOS \tilde{V}^{IG} , γ^{IG} iso- r_{KI}^{IG} curves

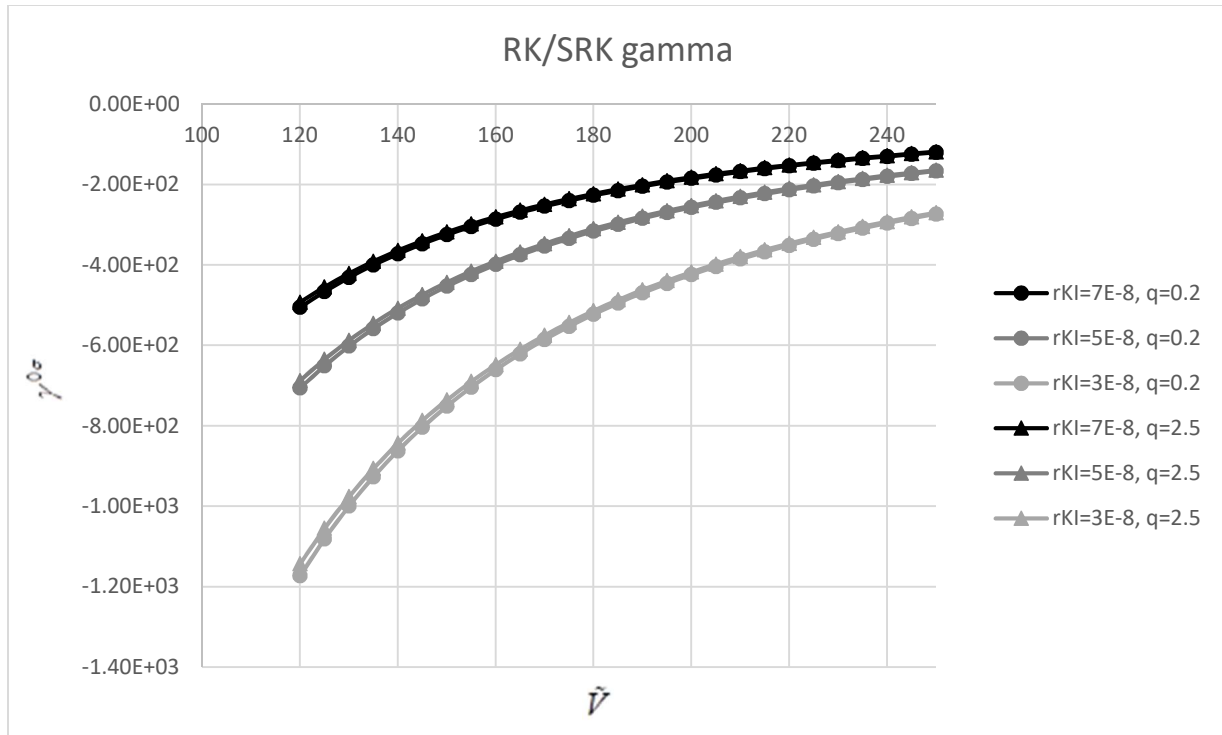


Figure 4: Redlich/Kwong, Soave/Redlich/Kwong DGCEOS $\tilde{V}, \gamma^{0\sigma}$ iso- (q, r_{KI}) curves

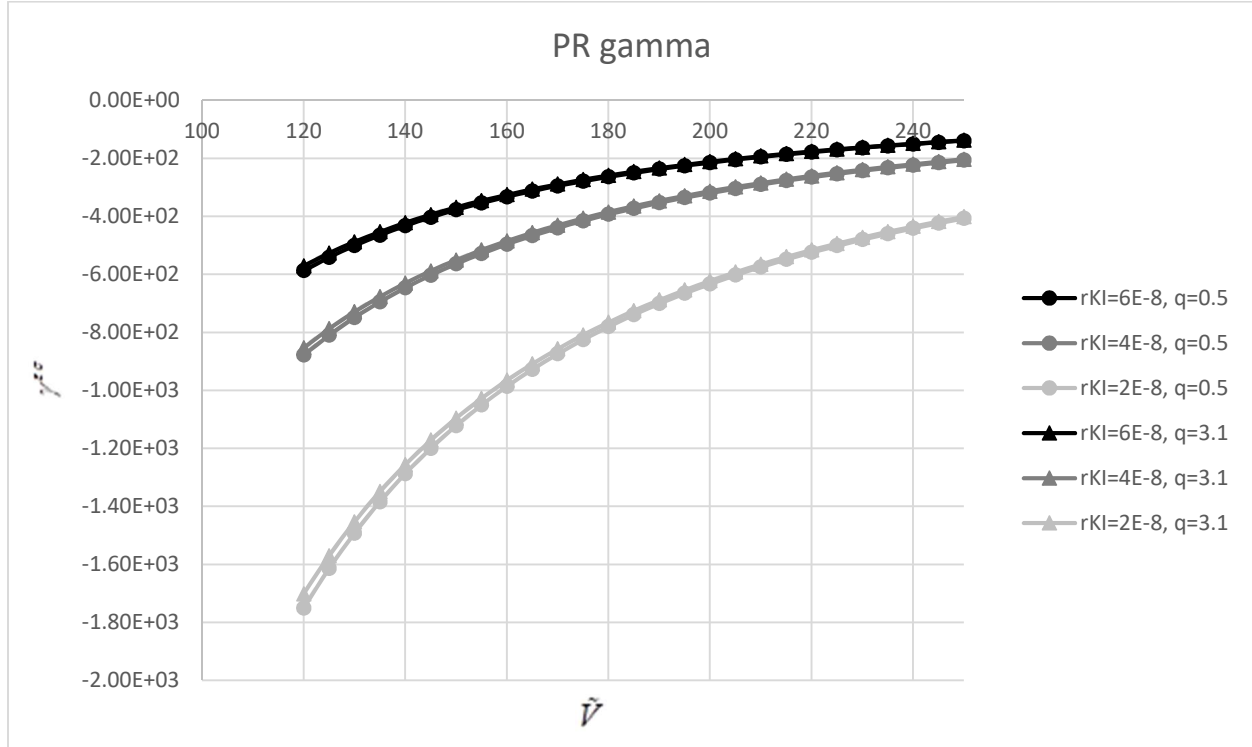


Figure 5: Peng/Robinson DGCEOS $\tilde{V}, \gamma^{\varepsilon\sigma}$ iso- (q, r_{KI}) curves

CH4/H2 Blend Pipeline Model and Case Studies

Two case studies will be conducted for H₂ containing mixtures: (1) CH₄/H₂ and (2) natural gas/H₂ (NG/H₂), with NG containing the following species: 95.124% CH₄, 1.438% N₂, 0.530% CO₂, 2.721% C₂H₆, 0.161% C₃H₈, 0.011% i-C₄H₁₀, 0.012% n-C₄H₁₀, 0.003% n-C₆H₁₄.

In carrying out these two case studies, the species data in Table 3 below will be used.

The species' molar masses, acentric factors, critical temperatures and pressures are obtained from [SVAS18, Table B.1, p.650]. The species' standard enthalpies of formation (at temperature 298.15 K (25 °C) and pressure 10⁵Pa) are obtained from [SVAS18, p. 147, Table C.4, p.658]. The value of the isobutane's standard enthalpy of formation is not included in the aforementioned reference. It is thus obtained from [Wik24] as follows. In SVAS18, p. 147, Table C.4 the enthalpy of formation of *n*-C₄H₁₀(g) is listed as -125,790 J/mol, while in [Wik24] the enthalpies of formation of *n*-C₄H₁₀(g) and *i*-C₄H₁₀(g) are listed as -125.5 J/mol and -134.3 J/mol respectively. Thus, considering the difference of the two enthalpies to be the important metric to be kept constant, the enthalpy of formation of *i*-C₄H₁₀(g) is listed as -134.590 J/mol.

The species' Lennard Jones potential related parameters $\sigma_i \left(\text{Å} \right)$, $\frac{\epsilon_i}{k} \left(\text{K} \right)$ are obtained from Table E.1 of [BSL07, p. 864-865].

Table 3: Species parameters

<i>Species i</i>	$M_i \left(\text{kg } i/\text{mol } i \right)$	ω_i	$T_{c,i} \left(\text{K} \right)$	$P_{c,i} \left(\text{bar} \right)$	$\Delta H_{f,i}^\circ \left(\text{J/mol } i \right)$	$\sigma_i \left(\text{Å} \right)$	$\frac{\epsilon_i}{k} \left(\text{K} \right)$
CH ₄ (g)	$16.043 \cdot 10^{-3}$	0.012	190.6	45.99	-74,520	3.780	154
H ₂ (g)	$2.016 \cdot 10^{-3}$	-0.216	33.19	13.13	0	2.915	38.0
O ₂ (g)	$31.999 \cdot 10^{-3}$	0.022	154.6	50.43	0	3.433	113
N ₂ (g)	$28.014 \cdot 10^{-3}$	0.038	126.2	34.00	0	3.667	99.8
CO ₂ (g)	$44.010 \cdot 10^{-3}$	0.224	304.2	73.83	-393,509	3.996	190
C ₂ H ₆ (g)	$30.070 \cdot 10^{-3}$	0.100	305.3	48.72	-83,820	4.388	232
C ₃ H ₈ (g)	$44.097 \cdot 10^{-3}$	0.152	369.8	42.48	-104,680	4.934	273
<i>i</i> -C ₄ H ₁₀ (g)	$58.123 \cdot 10^{-3}$	0.181	408.1	36.48	-134.590	5.393	295
<i>n</i> -C ₄ H ₁₀ (g)	$58.123 \cdot 10^{-3}$	0.200	425.1	37.96	-125,790	5.604	304
<i>n</i> -C ₆ H ₁₄ (g)	$86.177 \cdot 10^{-3}$	0.301	507.6	30.25	-166,920	6.264	342
H ₂ O(l)	$18.015 \cdot 10^{-3}$	0.345	647.1	220.55	-285,830	-	-

The case studies are carried out using the following data information and computational order, so that a non-hydrogen containing gas baseline prediction is created and compared to hydrogen containing gas related predictions:

Provided data: D_p , L_p , κ (pipeline diameter, length, surface roughness); $\{y_i\}_{i=1}^N$, T , \dot{m} , P_0 , (non-hydrogen containing gas species mole fractions, temperature, and mass flowrate throughout the pipeline, and inlet pressure).

Computational Order: The mass flowrates \dot{m} for all considered hydrogen blends are determined so that all the blends have the same power content, on a Joule per second and HHV basis, as the

baseline non-hydrogen containing gas for each case study. The molar mass M for all blends is calculated using the blends' $\{y_i\}_{i=1}^N$ and eqn. 5. b, b^{IG} are first computed for the IGEOS and GCEOS of all blends, using the blends' $\{y_i\}_{i=1}^N$ and eqns. 4, 6 respectively. $a(T), q$ are then computed for the GCEOS and DGCEOS of all blends, using the blends' $\{y_i\}_{i=1}^N$ and T and eqns. 4, 6, and $\beta_0^{IG}, \beta_0 = \Omega\beta_0^{IG}$ are computed for the DIGEOS, DGCEOS of all blends, using the blends' T , the calculated b, b^{IG} , the inlet pressure P_0 and eqn. 6. The dimensionless parameters $r_{KL}^{IG}, r_{KL} = \Omega^2 r_{KL}^{IG}$ are then computed using the pipeline D_p , the blends' $\{y_i\}_{i=1}^N$ and T , the calculated \dot{m}, M, b, b^{IG} and eqn. 15. The inlet dimensionless molar volumes $\tilde{V}_0^{IG}, \tilde{V}_0$ are then calculated using the calculated $\beta_0^{IG}, \beta_0 = \Omega\beta_0^{IG}, q$ and eqns. 9, 10. The $\frac{f}{r_{LD}}$ parameter in eqns. 16, 17 is calculated using the pipeline D_p, L_p and eq. 15 for $r_{LD}, \{y_i\}_{i=1}^N, T$ and eqn. 13 for $\mu(T)$, and D_p, κ and the calculated $\dot{m}, \mu(T)$ to calculate Re, f using eqn. 14. Then, $\frac{f}{r_{LD}}, \tilde{V}_0^{IG}, \tilde{V}_0, q, r_{KL}^{IG}, r_{KL} = \Omega^2 r_{KL}^{IG}$ and eqns. 16, 17 are used to calculate $\tilde{V}^{IG}(1), \tilde{V}(1)$. These quantities are then used to calculate $\beta^{IG}(1), \beta(1)$ using eqns 7, 8, and the IGEOS and GCEOS outlet P predictions using eqn. 6.

The above described computational order is partially illustrated in the IGEOS and GCEOS dependent tables below, which in going from the left to the right columns indicate the order in which the computations are executed, and from top to bottom their dependence on the mixture's hydrogen mole fraction.

CH4/H2 Case Study

The pressure drop prediction of the mechanical energy model studied in [BSL 15.4-2 example p.464-465] for pipeline transport of unblended pure CH₄ ($y_{H_2} = 0$) (considered as ideal gas) is used as a baseline for this case study. The relevant data are converted to SI units based on [RAP24], and all subsequent formula based variable/parameter evaluations are carried out using MS-Excel.

Pipeline information (diameter, length, roughness):

$$\left\{ \begin{array}{l} D_p = 2ft = 0.610m \\ L_p = 10mi. = 16093.4m \\ \kappa = 1 \cdot 10^{-5} m \end{array} \right\} \Rightarrow \left\{ \begin{array}{l} A_p = \pi \frac{D_p^2}{4} = \pi \frac{(0.610m)^2}{4} = 0.29225m^2 \\ r_{LD} = \frac{D_p}{L_p} = \frac{0.610m}{16093.4m} = 3.79037 \cdot 10^{-5} \\ \kappa/D_p = 1 \cdot 10^{-5}/0.610 = 1.64 \cdot 10^{-5} < 0.05 \end{array} \right\}$$

Pipeline CH₄ gas temperature: $T = 70^\circ F = 294.261K$

Pipeline CH₄ gas inlet pressure, mass flowrate: $P_0 = 100psia = 689476Pa, \dot{m} = 16.10967 \frac{kg CH_4}{s}$.

The mass flowrate is calculated using an inlet velocity of $v_0 = 40 \frac{ft}{s} = 12.192 \frac{m}{s}$, and employing the ideal gas assumption of the aforementioned baseline model.

Employing the above data then yields:

GCEOS Parameter accounting for molecule finite size:

$$\left\{ \begin{array}{l} b_{H_2}^{IG} = \frac{RT_{c,H_2}}{P_{c,H_2}} = \frac{8.314 \left(\frac{J}{mol \cdot K} \right) \cdot 33.19(K)}{1.313 \cdot 10^6(Pa)} = 2.1016 \cdot 10^{-4} \left(\frac{m^3}{mol} \right) \\ b_{CH_4}^{IG} = \frac{RT_{c,CH_4}}{P_{c,CH_4}} = \frac{8.314 \left(\frac{J}{mol \cdot K} \right) \cdot 190.6(K)}{4.599 \cdot 10^6(Pa)} = 3.4456 \cdot 10^{-4} \left(\frac{m^3}{mol} \right) \end{array} \right\} \Rightarrow$$

$$b^{IG} = \begin{bmatrix} 2.1016 \cdot 10^{-4} \cdot y_{H_2} + \\ + 3.4456 \cdot 10^{-4} \cdot (1 - y_{H_2}) \end{bmatrix}.$$

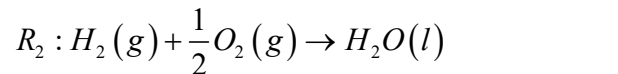
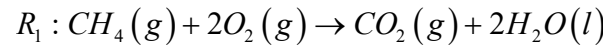
Pipeline CH₄ ideal gas inlet molar volume and dimensionless molar volume:

$$V_0^{IG} = \frac{RT}{P_0} = \frac{8.314 \left(\frac{J}{mol \cdot K} \right) \cdot 294.261(K)}{689476(Pa)} = 35.4833 \cdot 10^{-4} \left(\frac{m^3}{mol} \right),$$

$$\tilde{V}_0^{IG} = \frac{RT}{P_0 b^{IG}} = \frac{8.314 \left(\frac{J}{mol \cdot K} \right) \cdot 294.261(K)}{689476(Pa) \cdot 3.4456 \cdot 10^{-4} \left(\frac{m^3}{mol} \right)} = 10.2981$$

The mass flowrates for blends of CH₄/H₂ are determined based on the Higher Heating Value (HHV) on a mass basis. The HHV of a fuel is its standard heat of combustion at 25 °C with liquid water as a product.

The H₂ and CH₄ combustion reactions with liquid water as products are



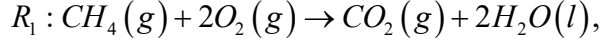
The standard heat of a reaction $R_j \ j = 1, M$, denoted as $\sum_{i=1}^N v_{ji} S_i = 0, j = 1, M$ with

$\{S_i\}_{i=1}^N, \{v_{ji}\}_{i=1}^N$ being the considered species and their stoichiometric coefficients in the

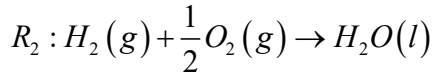
$R_j \ j = 1, M$ reaction respectively, with the latter being positive for products and negative for reactants, is expressed by the following equation:

$\Delta H_j^\circ = \sum_{i=1}^N v_{ji} \Delta H_{f,i}^\circ, j = 1, M$, where $\{\Delta H_{f,i}^\circ\}_{i=1}^N$ are the standard enthalpies of formation (at temperature 298.15 K (25 °C) and pressure 10⁵Pa) of the considered species.

The standard enthalpies of formation (at temperature 298.15 K (25 °C) and pressure 10⁵Pa) [SVAS18, p. 147, Table C.4, p.658] and molar masses [SVAS18, Table B.1, p.650] (for the species involved in the above reactions R_j , $j = 1, M = 2$ are:

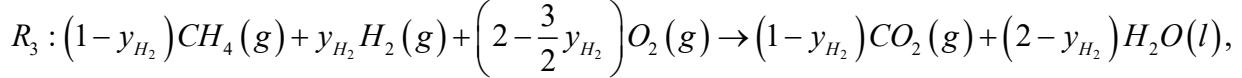


$$HHV_{molar} CH_4 = \Delta H_1^\circ = \left[(-1) \cdot (-74,520) + 0 \cdot 0 + (-2) \cdot 0 + (+1) \cdot (-393,509) + 2 \cdot (-285,830) + 0 \cdot (-241,818) \right] = -890,649 \left(\frac{J}{mol CH_4} \right)$$



$$HHV_{molar} H_2 = \Delta H_3^\circ = \left[0 \cdot (-74,520) + (-1) \cdot 0 + \left(\frac{-1}{2} \right) \cdot 0 + (+0) \cdot (-393,509) + (+1) \cdot (-285,830) + 0 \cdot (-241,818) \right] = -285,830 \left(\frac{J}{mol CH_4} \right)$$

Considering a H₂, CH₄ blend with the H₂, CH₄ mole fractions denoted as y_{H_2} , $y_{CH_4} = 1 - y_{H_2}$ then yields the following formula for the blend's HHV value on a molar basis:



$$HHV_{molar} blend = \Delta H_5^\circ = \left[-(1 - y_{H_2}) \cdot (-74,520) - y_{H_2} \cdot 0 - \left(2 - \frac{3}{2}y_{H_2} \right) \cdot 0 + +(1 - y_{H_2}) \cdot (-393,509) + (2 - y_{H_2}) \cdot (-285,830) + 0 \cdot (-241,818) \right] =$$

$$= [74,520 - 393,509 - 2 \cdot 285,830 + (285,830 + 393,509 - 74,520)y_{H_2}] \Rightarrow$$

$$HHV_{molar} blend = \left(-890,649 + 604,819y_{H_2} \right) \left(\frac{J}{mol blend} \right)$$

HHV values can be readily transformed from a molar basis to a mass basis through division with the average molar mass $M_{blend} \left(\frac{kg blend}{mol blend} \right)$ of the blend which is equal to:

$$M_{blend} \left(\frac{kg blend}{mol blend} \right) = y_{CH_4} \left(\frac{mol CH_4}{mol blend} \right) M_{CH_4} \left(\frac{kg CH_4}{mol CH_4} \right) + y_{H_2} \left(\frac{mol H_2}{mol blend} \right) M_{H_2} \left(\frac{kg H_2}{mol H_2} \right) = \\ = (1 - x_{H_2})16.043 \cdot 10^{-3} + y_{H_2} 2.016 \cdot 10^{-3} \Rightarrow$$

$$M_{blend} \left(\frac{kg blend}{mol blend} \right) = (16.043 \cdot 10^{-3} - 14.027 \cdot 10^{-3} y_{H_2})$$

Then, the blend's HHV value on a mass basis are:

$$HHV_{mass\ blend}\left(\frac{J}{kg\ blend}\right) = \frac{HHV_{molar\ blend}\left(\frac{J}{mol\ blend}\right)}{M_{blend}\left(\frac{kg\ blend}{mol\ blend}\right)} \Rightarrow$$

$$\boxed{HHV_{mass\ blend}\left(\frac{J}{kg\ blend}\right) = \frac{(-890,649 + 604,819y_{H_2})}{(16.043 \cdot 10^{-3} - 14.027 \cdot 10^{-3}y_{H_2})}}$$

Then the power content of the pure CH₄ pipeline inlet, on a Joule per second and HHV basis, is:

$$\dot{m} \cdot HHV_{mass\ blend} = 16.10967 \left(\frac{kg\ CH_4}{s} \right) \cdot \frac{(-890,649)}{(16.043 \cdot 10^{-3})} \left(\frac{J}{kg\ CH_4} \right) = -8.94350011 \cdot 10^8 \frac{J}{s} .$$

Then, the CH₄/H₂ blend mass flowrate $\dot{m}(y_{H_2})$ is determined as a function of the hydrogen mole fraction $y_{H_2} \neq 0$, so that the CH₄/H₂ blend's power content, on a Joule per second and HHV basis, is equal to that of the pure CH₄ pipeline inlet. Thus,

$$\dot{m}(y_{H_2}) \cdot \frac{(-890,649 + 604,819y_{H_2})}{(16.043 \cdot 10^{-3} - 14.027 \cdot 10^{-3}y_{H_2})} = \left(-8.94350011 \cdot 10^8 \frac{J}{s} \right) \Rightarrow$$

$$\boxed{\dot{m}(y_{H_2}) = (-8.94350011 \cdot 10^5) \frac{(16.043 - 14.027y_{H_2})}{(-890,649 + 604,819y_{H_2})}}$$

The species Lennard-Jones parameters provided in the above table, and the species viscosity relations provided earlier, yield the following relations for CH₄, H₂:

$$\left\{ \begin{array}{l}
\Omega_{\mu,H_2}(T) = \left[\begin{array}{l}
\frac{1.16145}{\left(\left(\frac{k}{\epsilon_i} \right)_{H_2} T \right)^{0.14874}} + \\
+ \frac{0.52487}{\exp \left(0.77320 \cdot \left(\frac{k}{\epsilon_i} \right)_{H_2} T \right)} + \\
+ \frac{2.16178}{\exp \left(2.43787 \cdot \left(\frac{k}{\epsilon_i} \right)_{H_2} T \right)}
\end{array} \right] = \left[\begin{array}{l}
\frac{1.16145}{\left(\frac{1}{38.0(K)} \cdot 294.261(K) \right)^{0.14874}} + \\
+ \frac{0.52487}{\exp \left(\frac{0.77320}{38.0(K)} \cdot 294.261(K) \right)} + \\
+ \frac{2.16178}{\exp \left(\frac{2.43787}{38.0(K)} \cdot 294.261(K) \right)}
\end{array} \right] = 0.857918 \\
\\
\Omega_{\mu,CH_4}(T) = \left[\begin{array}{l}
\frac{1.16145}{\left(\left(\frac{k}{\epsilon_i} \right)_{CH_4} T \right)^{0.14874}} + \\
+ \frac{0.52487}{\exp \left(0.77320 \cdot \left(\frac{k}{\epsilon_i} \right)_{CH_4} T \right)} + \\
+ \frac{2.16178}{\exp \left(2.43787 \cdot \left(\frac{k}{\epsilon_i} \right)_{CH_4} T \right)}
\end{array} \right] = \left[\begin{array}{l}
\frac{1.16145}{\left(\frac{1}{154(K)} \cdot 294.261(K) \right)^{0.14874}} + \\
+ \frac{0.52487}{\exp \left(\frac{0.77320}{154(K)} \cdot 294.261(K) \right)} + \\
+ \frac{2.16178}{\exp \left(\frac{2.43787}{154(K)} \cdot 294.261(K) \right)}
\end{array} \right] = 1.195096
\end{array} \right\}$$

$$\left\{ \begin{array}{l} \mu_{H_2}(T) = \frac{5}{16\sqrt{\pi}} \frac{\sqrt{M_{H_2}RT}}{N_A \sigma_{H_2}^2 \Omega_{\mu,H_2}(T)} = \frac{5}{16\sqrt{\pi}} \frac{\boxed{2.016 \cdot 10^{-3} \left(\frac{kg H_2}{mol H_2} \right) \cdot \\ \cdot 8.314 \left(\frac{J}{mol H_2 \cdot K} \right) \cdot \\ \cdot 294.261(K)}}{6.022 \cdot 10^{23} \left(\frac{1}{mol H_2} \right) \cdot \\ \cdot (2.915 \cdot 10^{-10} (m))^2 \cdot \\ \cdot 0.857918} = 8.9190 \cdot 10^{-6} \left(\frac{kg H_2}{m \cdot s} \right) \\ \\ \mu_{CH_4}(T) = \frac{5}{16\sqrt{\pi}} \frac{\sqrt{M_{CH_4}RT}}{N_A \sigma_{CH_4}^2 \Omega_{\mu,CH_4}(T)} = \frac{5}{16\sqrt{\pi}} \frac{\boxed{16.043 \cdot 10^{-3} \left(\frac{kg CH_4}{mol CH_4} \right) \cdot \\ \cdot 8.314 \left(\frac{J}{mol CH_4 \cdot K} \right) \cdot \\ \cdot 294.261(K)}}{6.022 \cdot 10^{23} \left(\frac{1}{mol CH_4} \right) \cdot \\ \cdot (3.780 \cdot 10^{-10} (m))^2 \cdot \\ \cdot 1.195096} = 1.0741 \cdot 10^{-5} \left(\frac{kg CH_4}{m \cdot s} \right) \end{array} \right.$$

Then from the mixing relations provided earlier, the CH₄/H₂ blend viscosity is:

$$\mu(T) = \frac{y_{H_2} \mu_{H_2}(T)}{y_{H_2} \Phi_{H_2,H_2}(T) + y_{CH_4} \Phi_{H_2,CH_4}(T)} + \frac{y_{CH_4} \mu_{CH_4}(T)}{y_{H_2} \Phi_{CH_4,H_2}(T) + y_{CH_4} \Phi_{CH_4,CH_4}(T)}$$

where:

$$\left\{
\begin{aligned}
\Phi_{H_2,H_2}(T) &= \frac{\left[1 + (\mu_{H_2}(T)/\mu_{H_2}(T))^{1/2} \cdot (M_{H_2}/M_{H_2})^{1/4}\right]^2}{\left[8(1 + (M_{H_2}/M_{H_2}))\right]^{1/2}} \\
\Phi_{CH_4,CH_4}(T) &= \frac{\left[1 + (\mu_{CH_4}(T)/\mu_{CH_4}(T))^{1/2} \cdot (M_{CH_4}/M_{CH_4})^{1/4}\right]^2}{\left[8(1 + (M_{CH_4}/M_{CH_4}))\right]^{1/2}} \\
\Phi_{H_2,CH_4}(T) &= \frac{\left[1 + (\mu_{H_2}(T)/\mu_{CH_4}(T))^{1/2} \cdot (M_{CH_4}/M_{H_2})^{1/4}\right]^2}{\left[8(1 + (M_{H_2}/M_{CH_4}))\right]^{1/2}} \\
\Phi_{CH_4,H_2}(T) &= \frac{\left[1 + (\mu_{CH_4}(T)/\mu_{H_2}(T))^{1/2} \cdot (M_{H_2}/M_{CH_4})^{1/4}\right]^2}{\left[8(1 + (M_{CH_4}/M_{H_2}))\right]^{1/2}}
\end{aligned}
\right\} \Rightarrow$$

$$\left\{
\begin{aligned}
\Phi_{H_2,H_2}(T) &= \frac{[1+1]^2}{[8(1+1)]^{1/2}} = 1, \quad \Phi_{CH_4,CH_4}(T) = \frac{[1+1]^2}{[8(1+1)]^{1/2}} = 1 \\
\Phi_{H_2,CH_4}(T) &= \frac{\left[1 + (8.9190 \cdot 10^{-6} / 1.0741 \cdot 10^{-5})^{1/2} \cdot (16.043 \cdot 10^{-3} / 2.016 \cdot 10^{-3})^{1/4}\right]^2}{\left[8(1 + (2.016 \cdot 10^{-3} / 16.043 \cdot 10^{-3}))\right]^{1/2}} = 2.1338 \\
\Phi_{CH_4,H_2}(T) &= \frac{\left[1 + (1.0741 \cdot 10^{-5} / 8.9190 \cdot 10^{-6})^{1/2} \cdot (2.016 \cdot 10^{-3} / 16.043 \cdot 10^{-3})^{1/4}\right]^2}{\left[8(1 + (16.043 \cdot 10^{-3} / 2.016 \cdot 10^{-3}))\right]^{1/2}} = 0.32292
\end{aligned}
\right\}.$$

Thus,

$$\mu(T)(y_{H_2}) = \left[\frac{y_{H_2} \cdot 8.9190 \cdot 10^{-6}}{y_{H_2} + (1 - y_{H_2}) \cdot 2.1338} + \frac{(1 - y_{H_2}) \cdot 1.0741 \cdot 10^{-5}}{y_{H_2} \cdot 0.32292 + (1 - y_{H_2})} \right] \left(\frac{kg \text{ blend}}{m \cdot s} \right)$$

The above relations $(y_{H_2}, \dot{m}(y_{H_2}))$, $(y_{H_2}, \mu(T)(y_{H_2}))$ are illustrated in Figure 6 below.

The flowrate $\dot{m}(y_{H_2})$ that delivers the same amount of HHV energy, is a monotonically decreasing function of y_{H_2} , while as shown in Appendix A2, the mixture viscosity exhibits a maximum at $y_{H_2} = 0.4613$ and is a monotonically increasing and decreasing function of y_{H_2} before and after $y_{H_2} = 0.4613$. This behavior of mixture viscosity is consistent with findings from the Aspen Hysys pipeline simulations of Abd et. al. [Abd21].

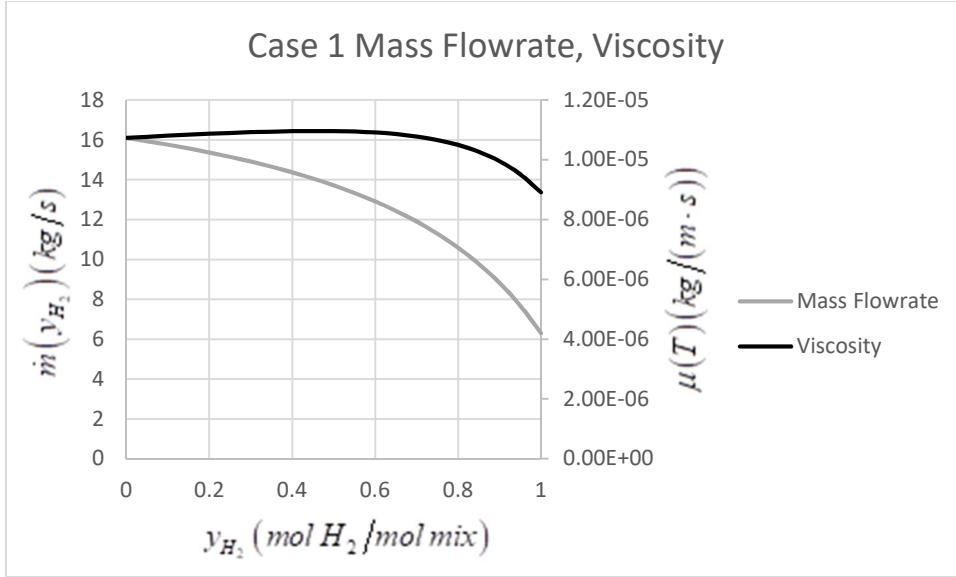


Figure 6: $(y_{H_2}, \dot{m}(y_{H_2}))$, $(y_{H_2}, \mu(T)(y_{H_2}))$ relations for Case 1 CH₄/H₂ mixture

For the baseline case, the pipeline CH₄ gas Reynolds number is:

$$Re = \frac{4\dot{m}}{\pi \cdot D_p \cdot \mu(T)} = \frac{4\dot{m}}{\pi \cdot D_p \cdot \mu_{CH_4}(T)} = \frac{4 \cdot 16.10967 \left(\frac{kg \cdot CH_4}{s} \right)}{\pi \cdot 0.610(m) \cdot 1.0741 \cdot 10^{-5} \left(\frac{kg \cdot CH_4}{m \cdot s} \right)} = 3.1305 \cdot 10^6$$

Pipeline CH₄ friction factor:

Since $4 \cdot 10^4 < Re < 10^8$ and, considering pipe roughness $\kappa = 1 \cdot 10^{-5}$,

$\kappa/D_p = 1 \cdot 10^{-5}/0.610 = 1.64 \cdot 10^{-5} < 0.05$, the Haaland friction factor model can be used.

$$\begin{aligned} \frac{1}{\sqrt{f}} &= -3.6 \cdot \log_{10} \left[\frac{6.9}{Re} + \left(\frac{(\kappa/D_p)^{10}}{3.7} \right)^{1/9} \right] \Rightarrow \\ f &= \left[-3.6 \cdot \log_{10} \left[\frac{6.9}{Re} + \left(\frac{(\kappa/D_p)^{10}}{3.7} \right)^{1/9} \right] \right]^{-2} = \left[-3.6 \cdot \log_{10} \left[\frac{6.9}{3.1305 \cdot 10^6} + \left(\frac{(1.64 \cdot 10^{-5})^{10}}{3.7} \right)^{1/9} \right] \right]^{-2} = 2.5717 \cdot 10^{-3} \end{aligned}$$

This friction factor value is consistent with the value $f = 2.5 \cdot 10^{-3}$ evaluated in [BSL 15.4-2 example p.464-465]. Then,

$$\frac{2f}{r_{LD}} = \frac{2f}{D_p/L_p} = \frac{2 \cdot 2.5717 \cdot 10^{-3}}{0.610/16093.4} = 1.3570 \cdot 10^2.$$

The resulting pressure drop model predictions for the considered EOS models and for various hydrogen mole fraction y_{H_2} values are:

IG:

y_H2	b (IG)	V~_0	rKI (IG)	V~(1)	P(1)	ΔP
0	0.000345	10.29803	9.19E-06	12.010598	591164.82	-98311.18
0.05	0.000338	10.50287	9.055E-06	12.307656	588371.61	-101104.4
0.1	0.000331	10.71602	8.916E-06	12.620357	585438.33	-104037.7
0.15	0.000324	10.93801	8.776E-06	12.949927	582358.12	-107117.9
0.2	0.000318	11.16939	8.633E-06	13.297694	579124.78	-110351.2
0.25	0.000311	11.41077	8.487E-06	13.665092	575733.29	-113742.7
0.3	0.000304	11.66281	8.338E-06	14.053646	572180.68	-117295.3
0.35	0.000298	11.92623	8.184E-06	14.464954	568467.17	-121008.8
0.4	0.000291	12.20183	8.025E-06	14.900642	564597.97	-124878
0.45	0.000284	12.49048	7.859E-06	15.36229	560585.9	-128890.1
0.5	0.000277	12.7931	7.685E-06	15.851295	556455.35	-133020.6
0.55	0.000271	13.11076	7.5E-06	16.368645	552248.17	-137227.8
0.6	0.000264	13.44459	7.301E-06	16.914549	548032.6	-141443.4
0.65	0.000257	13.79587	7.085E-06	17.487816	543917.06	-145558.9
0.7	0.00025	14.166	6.846E-06	18.08486	540071.34	-149404.7
0.75	0.000244	14.55653	6.577E-06	18.698077	536759.95	-152716.1
0.8	0.000237	14.96921	6.267E-06	19.313268	534394.77	-155081.2
0.85	0.00023	15.40597	5.901E-06	19.905648	533619.62	-155856.4
0.9	0.000224	15.86898	5.456E-06	20.433917	535447	-154029
0.95	0.000217	16.36068	4.898E-06	20.832269	541481.96	-147994
1	0.00021	16.88383	4.172E-06	21.001429	554295.48	-135180.5

RK:

y_H2	b (RK)	V~_0	rKI (RK)	a(T)	q	V~(1)	P(1)	ΔP
0	2.99E-05	117.2977	7.085E-08	0.1878509	2.5720692	137.38579	589790.3	-99685.7
0.05	2.93E-05	119.8161	6.979E-08	0.1733133	2.4202209	141.02749	586792.2	-102684
0.1	2.87E-05	122.4278	6.872E-08	0.159361	2.2705499	144.85186	583649.6	-105826
0.15	2.81E-05	125.1386	6.764E-08	0.1459942	2.1231915	148.8735	580355.5	-109121
0.2	2.75E-05	127.955	6.654E-08	0.1332128	1.9782926	153.10824	576903.3	-112573
0.25	2.69E-05	130.8837	6.541E-08	0.1210168	1.8360124	157.57313	573287.9	-116188
0.3	2.64E-05	133.9324	6.426E-08	0.1094062	1.6965246	162.28633	569506.2	-119970
0.35	2.58E-05	137.1092	6.308E-08	0.098381	1.5600185	167.26689	565558.3	-123918
0.4	2.52E-05	140.4231	6.185E-08	0.0879412	1.4267006	172.53414	561449.7	-128026
0.45	2.46E-05	143.8838	6.057E-08	0.0780868	1.2967972	178.10683	557193.8	-132282
0.5	2.4E-05	147.5022	5.923E-08	0.0688179	1.1705566	184.00141	552816	-136660
0.55	2.34E-05	151.2898	5.781E-08	0.0601343	1.0482515	190.2293	548359.8	-141116
0.6	2.29E-05	155.2599	5.628E-08	0.0520362	0.9301827	196.7922	543896.4	-145580
0.65	2.23E-05	159.4266	5.461E-08	0.0445234	0.8166821	203.67458	539538.8	-149937

0.7	2.17E-05	163.8059	5.277E-08	0.0375961	0.7081175	210.83121	535464.2	-154012
0.75	2.11E-05	168.4153	5.069E-08	0.0312542	0.604897	218.16723	531948.4	-157528
0.8	2.05E-05	173.2746	4.83E-08	0.0254977	0.5074752	225.50638	529420.9	-160055
0.85	2E-05	178.4055	4.548E-08	0.0203266	0.4163596	232.54203	528552.6	-160923
0.9	1.94E-05	183.8326	4.205E-08	0.0157409	0.3321189	238.76545	530397.5	-159079
0.95	1.88E-05	189.5835	3.775E-08	0.0117406	0.2553921	243.37106	536622.8	-152853
1	1.82E-05	195.6892	3.216E-08	0.0083257	0.1868999	245.15567	549890.7	-139585

SRK:

y_H2	b (SRK)	V~_0	rKI		q	V~(1)	P(1)	ΔP
			(SRK)	a(T)				
0	2.99E-05	117.4022	7.072E-08	0.1803472	2.4693281	137.46803	589883.8	-99592.2
0.05	2.93E-05	119.8985	6.967E-08	0.1674937	2.3389538	141.08121	586909.8	-102566
0.1	2.87E-05	122.489	6.86E-08	0.1551153	2.2100573	144.87749	583791.4	-105685
0.15	2.81E-05	125.1795	6.752E-08	0.143212	2.0827303	148.87147	580521.2	-108955
0.2	2.75E-05	127.9763	6.642E-08	0.1317839	1.9570724	153.07897	577092.9	-112383
0.25	2.69E-05	130.8865	6.53E-08	0.1208309	1.8331919	157.51703	573501.3	-115975
0.3	2.64E-05	133.9177	6.415E-08	0.110353	1.7112065	162.20384	569743.1	-119733
0.35	2.58E-05	137.078	6.297E-08	0.1003502	1.5912447	167.15842	565818.7	-123657
0.4	2.52E-05	140.3764	6.174E-08	0.0908226	1.4734467	172.40017	561733.2	-127743
0.45	2.46E-05	143.8228	6.047E-08	0.0817701	1.3579661	177.94785	557499.9	-131976
0.5	2.4E-05	147.4281	5.913E-08	0.0731928	1.2449714	183.81799	553144.2	-136332
0.55	2.34E-05	151.2039	5.77E-08	0.0650905	1.1346476	190.02212	548709.2	-140767
0.6	2.29E-05	155.1635	5.618E-08	0.0574634	1.0271989	196.56217	544265.9	-145210
0.65	2.23E-05	159.3213	5.451E-08	0.0503115	0.9228506	203.42289	539926.8	-149549
0.7	2.17E-05	163.6932	5.268E-08	0.0436346	0.8218522	210.55959	535868.2	-153608
0.75	2.11E-05	168.297	5.06E-08	0.0374329	0.7244808	217.87818	532365	-157111
0.8	2.05E-05	173.1524	4.822E-08	0.0317063	0.6310448	225.20366	529845.2	-159631
0.85	2E-05	178.2814	4.54E-08	0.0264549	0.5418888	232.23129	528977.5	-160498
0.9	1.94E-05	183.7089	4.198E-08	0.0216786	0.4573987	238.45507	530812.7	-158663
0.95	1.88E-05	189.4624	3.768E-08	0.0173774	0.3780081	243.07302	537013.7	-152462
1	1.82E-05	195.5734	3.21E-08	0.0135513	0.3042062	244.88609	550236.3	-139240

PR:

y_H2	b (PR)	V~_0	rKI (PR)	a(T)	q	V~(1)	P(1)	ΔP
0	2.68E-05	130.2714	5.744E-08	0.2043238	3.115496	152.71522	589505.6	-99970.4
0.05	2.63E-05	133.0505	5.658E-08	0.1910539	2.9711047	156.74644	586511.5	-102964
0.1	2.58E-05	135.9348	5.572E-08	0.1782295	2.8279213	160.98297	583371.5	-106105
0.15	2.52E-05	138.931	5.484E-08	0.1658506	2.6860207	165.44121	580078.1	-109398
0.2	2.47E-05	142.0461	5.395E-08	0.1539171	2.5454843	170.13893	576624.9	-112851
0.25	2.42E-05	145.288	5.303E-08	0.1424292	2.4064007	175.09532	573006.4	-116470
0.3	2.37E-05	148.6652	5.21E-08	0.1313868	2.2688661	180.33084	569219.4	-120257
0.35	2.31E-05	152.1867	5.114E-08	0.1207899	2.1329854	185.86691	565264	-124212

0.4	2.26E-05	155.8627	5.015E-08	0.1106384	1.9988733	191.72537	561145.4	-128331
0.45	2.21E-05	159.7042	4.911E-08	0.1009325	1.8666554	197.92738	556876.8	-132599
0.5	2.16E-05	163.7233	4.802E-08	0.0916721	1.7364692	204.49162	552483.4	-136993
0.55	2.11E-05	167.9331	4.687E-08	0.0828571	1.6084662	211.43113	548008.9	-141467
0.6	2.05E-05	172.3484	4.563E-08	0.0744877	1.4828131	218.74816	543524.3	-145952
0.65	2E-05	176.9853	4.428E-08	0.0665638	1.3596941	226.42566	539142.9	-150333
0.7	1.95E-05	181.8616	4.278E-08	0.0590853	1.2393131	234.41338	535042.2	-154434
0.75	1.9E-05	186.9972	4.11E-08	0.0520524	1.1218967	242.60541	531499.1	-157977
0.8	1.84E-05	192.4141	3.916E-08	0.045465	1.0076969	250.8046	528944.7	-160531
0.85	1.79E-05	198.1371	3.687E-08	0.039323	0.8969953	258.66749	528053.1	-161423
0.9	1.74E-05	204.1937	3.409E-08	0.0336266	0.7901074	265.62389	529883.3	-159593
0.95	1.69E-05	210.6149	3.061E-08	0.0283757	0.6873875	270.77066	536110.7	-153365
1	1.64E-05	217.4358	2.607E-08	0.0235702	0.5892356	272.75963	549410.2	-140066

The above results demonstrate that the pipeline pressure drop exhibits a minimum at $y_{H_2} = 0.85$ and is a monotonically decreasing and increasing function of y_{H_2} before and after $y_{H_2} = 0.85$. This is illustrated in Figure 7, which also demonstrates differences in pressure drop predictions of up to 3.045% between IGEOS and GCEOS. For $y_{H_2} = 0$, the IGEOS pressure drop prediction is identical to the baseline case in [BSL 15.4-2 example p.464-465], while the GCEOS pressure drop predictions for $y_{H_2} = 0$ are different at about 0.147% to 1.61%.

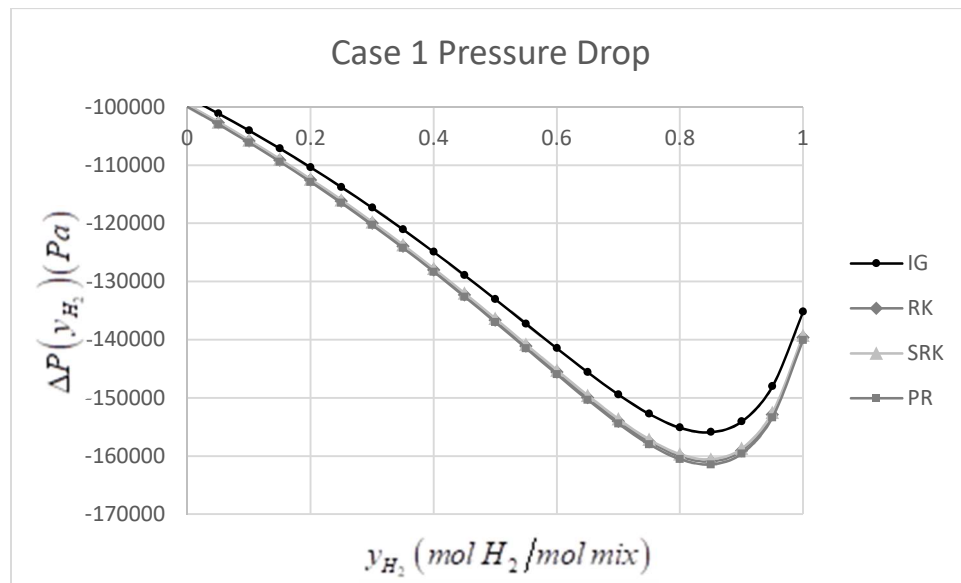


Figure 7: $(y_{H_2}, \Delta P(y_{H_2}))$ relations for Case 1 CH₄/H₂ mixture, IGEOS, GCEOS

NG/H2 Case Study

For this case study we employ information provided by a natural gas (NG) pipeline owning company regarding a realistic NG composition and NG pipeline and NG feed data, [Com24]. NG contains 8 species and has the following composition (in mole fraction $\{y_i\}_{i=1}^N$ terms): 95.124%

CH_4 , 1.438% N_2 , 0.530% CO_2 , 2.721% C_2H_6 , 0.161% C_3H_8 , 0.011% i- C_4H_{10} , 0.012% n- C_4H_{10} , 0.003% n- C_6H_{14} .

The pipeline NG gas inlet pressure and velocity are:

$$P_0 = 734.56 \text{ psia} = 5064612.92 \text{ Pa}, v_0 = 258.11 \frac{\text{m}}{\text{s}}$$

The pipeline NG gas temperature is: $T = 83.35^\circ\text{F} = 301.483\text{K}$

The pipeline dimensions are:

$$\left\{ \begin{array}{l} D_p = 33.162 \text{ in.} = 0.8423148 \text{ m} \\ L_p = 24.31 \text{ mi.} = 39121.903 \text{ m} \end{array} \right\} \Rightarrow \left\{ \begin{array}{l} A_p = \pi \frac{D_p^2}{4} = \pi \frac{(0.8423148 \text{ m})^2}{4} = 0.5572355 \text{ m}^2 \\ r_{LD} = \frac{D_p}{L_p} = \frac{0.8423148 \text{ m}}{39121.903 \text{ m}} = 2.15305 \cdot 10^{-5} \end{array} \right\}$$

The pipeline NG gas inlet mass flow rate is: $\dot{m} = 102.36 \frac{\text{kg NG}}{\text{s}}$

Then, the pipeline NG gas inlet mass density is:

$$\rho_{0,NG} = \frac{\dot{m}}{v_0 A_p} = \frac{102.36 \left(\frac{\text{kg NG}}{\text{s}} \right)}{258.11 \left(\frac{\text{m}}{\text{s}} \right) 0.5572355 \left(\text{m}^2 \right)} = 0.7116831 \left(\frac{\text{kg NG}}{\text{m}^3 \text{ NG}} \right)$$

For the provided NG composition of 8 species, the NG molar mass is

$$M_{NG} \left(\frac{\text{kg NG}}{\text{mol NG}} \right) = 16.8019915 \cdot 10^{-3} \left(\frac{\text{kg NG}}{\text{mol NG}} \right)$$

Then, the pipeline NG gas inlet molar volume is

$$V_0 \left(\frac{\text{m}^3 \text{ NG}}{\text{mol NG}} \right) = \frac{M_{NG} \left(\frac{\text{kg NG}}{\text{mol NG}} \right)}{\rho_{0,NG} \left(\frac{\text{kg NG}}{\text{m}^3 \text{ NG}} \right)} = \frac{16.8019915 \cdot 10^{-3} \left(\frac{\text{m}^3 \text{ NG}}{\text{mol NG}} \right)}{0.7116831} = 0.023609 \left(\frac{\text{m}^3 \text{ NG}}{\text{mol NG}} \right).$$

The above information will help determine which of the IGEOS, GCEOS model molar volume predictions at the pipeline entrance are closest to the above molar volume calculated by the provided inlet data. In creating the NG/ H_2 blend composition ((in mole fraction $\{y_i\}_{i=1}^N$ terms), it is considered that the mole fraction ratios of the 8 species in NG are kept constant for any NG/ H_2 blend. The mass flowrates for blends of NG/ H_2 are determined based on the Higher Heating Value (HHV) on a mass basis.

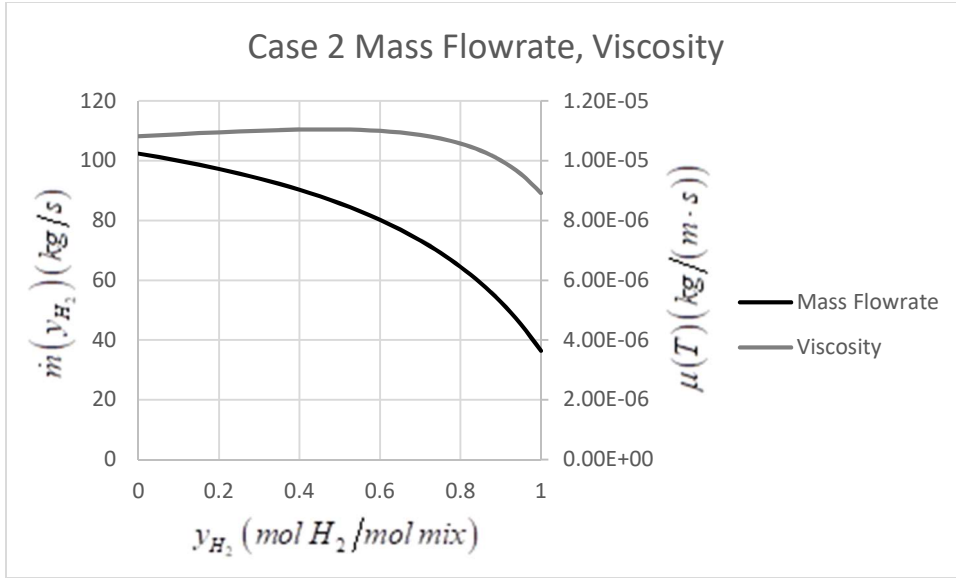


Figure 8: $(y_{H_2}, \dot{m}(y_{H_2}))$, $(y_{H_2}, \mu(T)(y_{H_2}))$ relations for Case 2 NG/H₂ mixture

The resulting pressure drop model predictions for the considered EOS models and for various hydrogen mole fraction y_{H_2} values are:

IG:

y_{H2}	b (IG)	$V \sim 0$	rKI (IG)	$V \sim (1)$	P(1)	ΔP
0	0.000349613	1.415594	9.79325E-05	1.476607	4855343.564	-209269.356
0.05	0.000342641	1.444401	9.61947E-05	1.508216	4850320.683	-214292.2373
0.1	0.000335668	1.474404	9.44312E-05	1.541201	4845110.383	-219502.5367
0.15	0.000328695	1.505681	9.26376E-05	1.575650	4839712.426	-224900.4943
0.2	0.000321723	1.538313	9.08086E-05	1.611657	4834129.92	-230482.9996
0.25	0.00031475	1.572391	8.89377E-05	1.649325	4828370.715	-236242.205
0.3	0.000307778	1.608013	8.70172E-05	1.688761	4822449.316	-242163.6041
0.35	0.000300805	1.645286	8.50375E-05	1.730080	4816389.566	-248223.3541
0.4	0.000293832	1.684329	8.29863E-05	1.773403	4810228.402	-254384.5178
0.45	0.00028686	1.725269	8.08488E-05	1.818856	4804021.175	-260591.7448
0.5	0.000279887	1.768249	7.86057E-05	1.866565	4797849.249	-266763.6713
0.55	0.000272915	1.813426	7.62326E-05	1.916658	4791830.98	-272781.9404
0.6	0.000265942	1.860971	7.36977E-05	1.969249	4786137.78	-278475.1401
0.65	0.000258969	1.911077	7.09595E-05	2.024436	4781017.941	-283594.9789
0.7	0.000251997	1.963955	6.79625E-05	2.082274	4776832.536	-287780.3842
0.75	0.000245024	2.019843	6.46317E-05	2.142749	4774110.487	-290502.4329
0.8	0.000238052	2.079005	6.08638E-05	2.205731	4773634.751	-290978.1692
0.85	0.000231079	2.141737	5.65133E-05	2.270886	4776580.312	-288032.6077
0.9	0.000224106	2.208372	5.13706E-05	2.337546	4784741.086	-279871.8343
0.95	0.000217134	2.279288	4.51258E-05	2.404481	4800915.07	-263697.8505
1	0.000210161	2.354909	3.73046E-05	2.469508	4829586.018	-235026.9023

RK:

y_H2	b (RK)	V~_0	rKI (RK)	a(T)	q	V~(1)	P(1)	ΔP
0	3.029E-05	14.895372	7.351E-07	0.193469	2.548191	15.529376	4873876	-190736.9
0.05	2.9686E-05	15.390995	7.221E-07	0.178416	2.397748	16.062629	4866825	-197787.9
0.1	2.9082E-05	15.894320	7.088E-07	0.163973	2.249417	16.605836	4859648	-204964.8
0.15	2.8478E-05	16.406639	6.954E-07	0.150139	2.103333	17.160430	4852341	-212272.3
0.2	2.7874E-05	16.929239	6.817E-07	0.136915	1.95964	17.727840	4844902	-219710.7
0.25	2.727E-05	17.463426	6.676E-07	0.124300	1.818499	18.309504	4837339	-227274.3
0.3	2.6666E-05	18.010538	6.532E-07	0.112295	1.680083	18.906878	4829663	-234950.1
0.35	2.6062E-05	18.571965	6.383E-07	0.100899	1.544581	19.521439	4821899	-242714
0.4	2.5458E-05	19.149164	6.229E-07	0.090113	1.4122	20.154677	4814085	-250528.1
0.45	2.4854E-05	19.743679	6.069E-07	0.079936	1.283169	20.808085	4806279	-258334.4
0.5	2.4249E-05	20.357157	5.901E-07	0.070370	1.157738	21.483127	4798566	-266047.1
0.55	2.3645E-05	20.991365	5.722E-07	0.061412	1.036182	22.181184	4791072	-273541.3
0.6	2.3041E-05	21.648218	5.532E-07	0.053064	0.918806	22.903471	4783977	-280636.2
0.65	2.2437E-05	22.329795	5.327E-07	0.045326	0.805949	23.650888	4777543	-287070.3
0.7	2.1833E-05	23.038371	5.102E-07	0.038197	0.697984	24.423793	4772149	-292464.1
0.75	2.1229E-05	23.776445	4.852E-07	0.031678	0.595331	25.221631	4768349	-296263.4
0.8	2.0625E-05	24.546778	4.569E-07	0.025768	0.498454	26.042332	4766963	-297649.8
0.85	2.0021E-05	25.352434	4.242E-07	0.020468	0.407879	26.881328	4769215	-295398.1
0.9	1.9417E-05	26.196827	3.856E-07	0.015778	0.324191	27.729930	4776970	-287642.6
0.95	1.8812E-05	27.083781	3.387E-07	0.011697	0.248056	28.572606	4793133	-271480
1	1.8208E-05	28.017596	2.8E-07	0.008225	0.180225	29.382325	4822344	-242268.6

SRK:

y_H2	b (SRK)	V~_0	rKI (SRK)	a(T)	q	V~(1)	P(1)	ΔP
0	3.029E-05	14.036102	7.351E-07	0.248463	3.272527	14.637047	4884854	-179758.7
0.05	2.9686E-05	14.534375	7.221E-07	0.233569	3.138961	15.171251	4877814	-186799.1
0.1	2.9082E-05	15.040334	7.088E-07	0.219136	3.00616	15.715412	4870646	-193966.8
0.15	2.8478E-05	15.555469	6.954E-07	0.205163	2.874174	16.271159	4863343	-201269.5
0.2	2.7874E-05	16.081245	6.817E-07	0.191650	2.743055	16.840101	4855902	-208710.6
0.25	2.727E-05	16.619128	6.676E-07	0.178597	2.612861	17.423847	4848325	-216287.5
0.3	2.6666E-05	17.170612	6.532E-07	0.166004	2.483655	18.024016	4840623	-223990.1
0.35	2.6062E-05	17.737238	6.383E-07	0.153872	2.355505	18.642252	4832815	-231798.3
0.4	2.5458E-05	18.320619	6.229E-07	0.142200	2.228487	19.280217	4824935	-239677.8
0.45	2.4854E-05	18.922455	6.069E-07	0.130989	2.102683	19.939589	4817038	-247575.2
0.5	2.4249E-05	19.544558	5.901E-07	0.120238	1.978184	20.622029	4809203	-255410.2
0.55	2.3645E-05	20.188874	5.722E-07	0.109947	1.85509	21.329140	4801549	-263063.9
0.6	2.3041E-05	20.857507	5.532E-07	0.100116	1.733512	22.062380	4794250	-270363.3
0.65	2.2437E-05	21.552744	5.327E-07	0.090746	1.613571	22.822934	4787557	-277055.9
0.7	2.1833E-05	22.277092	5.102E-07	0.081836	1.495405	23.611482	4781839	-282773.8
0.75	2.1229E-05	23.033304	4.852E-07	0.073386	1.379163	24.427850	4777636	-286976.7

0.8	2.0625E-05	23.824429	4.569E-07	0.065397	1.265016	25.270415	4775749	-288863.9
0.85	2.0021E-05	24.653850	4.242E-07	0.057868	1.153154	26.135140	4777380	-287232.8
0.9	1.9417E-05	25.525348	3.856E-07	0.050799	1.043788	27.013973	4784366	-280246.7
0.95	1.8812E-05	26.443161	3.387E-07	0.044191	0.93716	27.892147	4799573	-265039.6
1	1.8208E-05	27.412066	2.8E-07	0.038043	0.833543	28.743544	4827594	-237018.9

PR:

y_H2	b (SRK)	V~_0	rKI (SRK)	a(T)	q	V~(1)	P(1)	ΔP
0	2.72E-05	15.393815	5.928E-07	0.263982	3.871987	16.048250	4887607	-177006.3
0.05	2.6657E-05	15.978765	5.823E-07	0.246719	3.692424	16.674327	4880229	-184384.1
0.1	2.6115E-05	16.570250	5.716E-07	0.230040	3.514317	17.309481	4872744	-191868.6
0.15	2.5573E-05	17.170171	5.607E-07	0.213945	3.337761	17.955770	4865143	-199470.2
0.2	2.503E-05	17.780343	5.496E-07	0.198433	3.162855	18.615170	4857419	-207194.1
0.25	2.4488E-05	18.402542	5.383E-07	0.183505	2.989709	19.289616	4849574	-215039
0.3	2.3945E-05	19.038540	5.267E-07	0.169160	2.818443	19.981019	4841617	-222996
0.35	2.3403E-05	19.690137	5.147E-07	0.155400	2.649188	20.691289	4833568	-231045.4
0.4	2.286E-05	20.359184	5.023E-07	0.142223	2.482086	21.422336	4825460	-239153.3
0.45	2.2318E-05	21.047613	4.894E-07	0.129629	2.317296	22.176059	4817347	-247266.3
0.5	2.1775E-05	21.757463	4.758E-07	0.117620	2.154988	22.954326	4809309	-255303.5
0.55	2.1233E-05	22.490905	4.614E-07	0.106194	1.995355	23.758917	4801467	-263145.6
0.6	2.069E-05	23.250269	4.461E-07	0.095352	1.838606	24.591436	4793995	-270618.1
0.65	2.0148E-05	24.038076	4.295E-07	0.085093	1.684974	25.453156	4787146	-277467.2
0.7	1.9605E-05	24.857074	4.114E-07	0.075418	1.534718	26.344776	4781290	-283322.5
0.75	1.9063E-05	25.710272	3.912E-07	0.066327	1.388126	27.266011	4776972	-287640.8
0.8	1.852E-05	26.600986	3.684E-07	0.057820	1.24552	28.214940	4774996	-289617.4
0.85	1.7978E-05	27.532892	3.421E-07	0.049896	1.107261	29.186920	4776568	-288044.6
0.9	1.7435E-05	28.510081	3.109E-07	0.042556	0.973755	30.172795	4783534	-281078.6
0.95	1.6893E-05	29.537134	2.731E-07	0.035799	0.845459	31.155882	4798768	-265844.6
1	1.6351E-05	30.619202	2.258E-07	0.029626	0.722892	32.106798	4826875	-237737.7

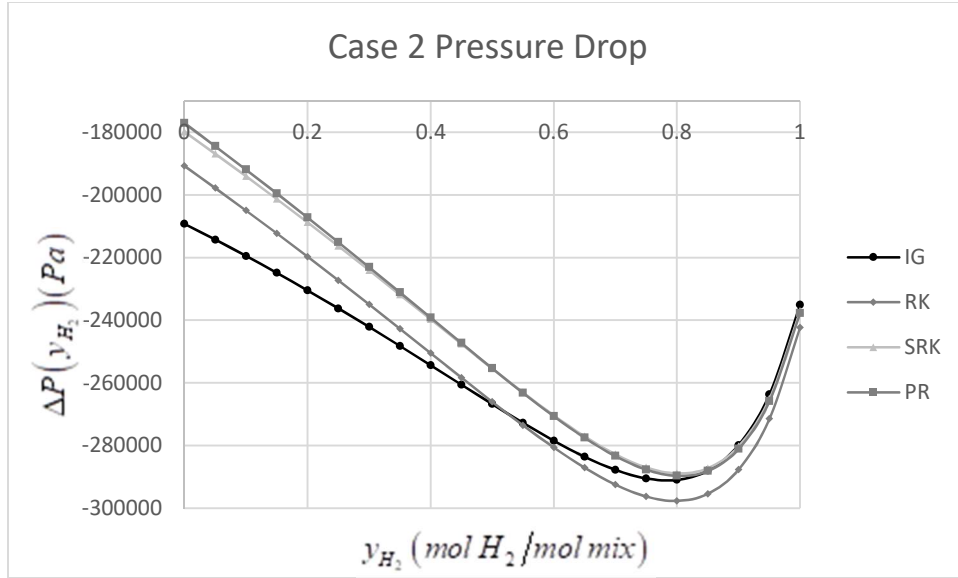


Figure 9: $(y_{H_2}, \Delta P(y_{H_2}))$ relations for Case 2 NG/H₂ mixture, IGEOS, GCEOS

Conclusions:

In this work, we presented a novel, dimensionless model that results in a dimensionless algebraic equation parametrized with only three dimensionless temperature, geometry, and flow related parameters r_{KI}, q, r_{LD} , thus providing the potential for parametric studies in a parameter space of reduced dimension compared to the parameter space of dimensional models. We quantified the pressure drop dependence on hydrogen mole fraction of a binary, methane hydrogen mixture, and a natural gas hydrogen mixture with a real life natural gas composition containing eight species using the IG and nonideal GCEOS, for steady state, isothermal, compressible flow through a straight, horizontal pipeline. Our calculations showed excellent agreement with simulations and calculations from prior works focusing on pure methane and methane-hydrogen blends.

References

- [Abb21] Abbas, A. J., Hassani, H., Burby, M., & John, I. J. An investigation into the volumetric flow rate requirement of hydrogen transportation in existing natural gas pipelines and its safety implications. *Gases*, 1(4), 156-179, (2021).
- [Abd21] Abd, A. A., Naji, S. Z., Thian, T. C., & Othman, M. R. Evaluation of hydrogen concentration effect on the natural gas properties and flow performance. *International Journal of Hydrogen Energy*, 46(1), 974-983, (2021)
- [All21] Allison, TC, Klaerner, J, Cich, S, Kurz, R, & McBain, M. "Power and Compression Analysis of Power-To-Gas Implementations in Natural Gas Pipelines With Up to 100% Hydrogen Concentration." Proceedings of the ASME Turbo Expo 2021: Turbomachinery Technical Conference and Exposition. Volume 8: Oil and Gas Applications; Steam Turbine. Virtual, Online. June 7–11, (2021)

- [Bai19] Bainier, F., Kurz, R. "Impacts of H₂ Blending on Capacity and Efficiency on a Gas Transport Network." Proceedings of the ASME Turbo Expo 2019: Turbomachinery Technical Conference and Exposition. Volume 9: Oil and Gas Applications; Supercritical CO₂ Power Cycles; Wind Energy. Phoenix, Arizona, USA. June 17–21, (2019)
- [BSL02] Bird RB, Stewart WE, Lightfoot EN. "Transport Phenomena" Revised 2nd ed. John Wiley and Sons, Inc. (2002)
- [BSL07] Bird RB, Stewart WE, Lightfoot EN. "Transport Phenomena" Revised 2nd ed. John Wiley and Sons, Inc. (2007)
- [Com24] Personal Communication from natural gas (NG) pipeline owning company
- [Cri23] Cristello, J. B., Yang, J. M., Hugo, R., Lee, Y., & Park, S. S. Feasibility analysis of blending hydrogen into natural gas networks. International Journal of Hydrogen Energy, 48(46), 17605–17629, (2023)
- [DeN05] de Nevers N. "Fluid Mechanics for Chemical Engineers" 3rd ed. McGraw-Hill (2005)
- [KCG03] Bird RB, Stewart WE, Lightfoot EN. "Chemically Reacting Flow Theory and Practice" 2nd ed. John Wiley and Sons, Inc. (2003)
- [Li21] Li, J., Su, Y., Yu, B., Wang, P., & Sun, D. Influences of hydrogen blending on the Joule–Thomson coefficient of natural gas. *ACS omega*, 6(26), 16722–16735, (2021)
- [NJA72], Neufeld PD, Janzen AR, Aziz RA. "Empirical Equations to calculate 16 of the Transport Collision Integrals $\Omega^{(I,s)*}$ for the Lennard-Jones (12-6) Potential" *J. Chem. Phys.* 57: 1100–1102 (1972)
- [RAP24] <https://www.rapidtables.com/convert/index.html>
- [SVAS22] Smith JM, Van Ness HC, Abbott MM, Swihart MT. "Introduction to Chemical Engineering Thermodynamics" 9th ed. McGraw-Hill (2022)
- [SI19] The International System of Units (SI) 9th edition 2019 V2.01 (December 2022)
- [Wil50] Wilke CR. "A Viscosity Equation for Gas Mixtures" *J. Chem. Phys.* 18 (4): 517–519 (1950)
- [Wik24] https://en.wikipedia.org/wiki/Standard_enthalpy_ofFormation
- [Wol24a]
<https://www.wolframalpha.com/input/?i2d=true&i=Integrate%5BDivide%5B%5C%2840%29-x%2B2%5C%2841%29%2CPower%5B%5C%2840%29x-1%5C%2841%29%2C2%5D%5D%2Cx%5D>
- [Wol24b]
https://www.wolframalpha.com/input/?i2d=true&i=Integrate%5BDivide%5B%5C%2840%29-x-2*e%5C%2841%29%2CPower%5B%5C%2840%29x%2Be%5C%2841%29%2C2%5D%5D%2Cx%5D
- [Wol24c]
https://www.wolframalpha.com/input/?i=limit+as+x+approaches+infinity&assumption=%7B%22MC%22%2C+%22%22%7D+-%3E+%7B%22Calculator%22%2C+%22dflt%22%7D&assumption=%7B%22F%22%2C+%22AsymptoticLimitCalculator%22%2C+%22limitfunction%22%7D+-%3E%22-In%28x%29%2Bb*%28In%28x%2F%28x-1%29%29-%281%2F%28x-1%29%29%29%2Bc*%28ln%28x%2F%28a%2Bx%29%29%2B%281%2F%28a%2Bx%29%29

[%29%2B1%2F%282*a*x%5E2%29%22&assumption=%7B%22FP%22%2C+%22AsymptoticLimitCalculator%22%2C+%22limit%22%7D+-%3E+%22positive%22\]](#)

[Zha24] Zhang, B., Xu, N., Zhang, H., Qiu, R., Wei, X., Wang, Z., & Liang, Y. Influence of hydrogen blending on the operation of natural gas pipeline network considering the compressor power optimization. *Applied Energy*, 358, 122594, (2024)

Acknowledgement

Financial support through the California Energy Commission Grant PIR-22-003. “Pilot Testing and Assessment of Safety and Integrity of Targeted Hydrogen Blending in Gas Infrastructure for Decarbonization” is gratefully acknowledged.

Appendix

A.1 Proof of Theorem

a. IGEOs:

$$\begin{aligned} M \left(\frac{4\dot{m}}{M \cdot \pi \cdot D_p^2} \right)^2 dV + M \left(\frac{2f}{D_p} \left(\frac{4\dot{m}}{M \cdot \pi \cdot D_p^2} \right)^2 V \right) dl + dP = 0 \Rightarrow \\ M \left(\frac{4\dot{m}}{M \cdot \pi \cdot D_p^2} \right)^2 \frac{b^{IG}}{RT} dV + M \left(\frac{2f}{D_p} \left(\frac{4\dot{m}}{M \cdot \pi \cdot D_p^2} \right)^2 V \right) \frac{b^{IG}}{RT} dl + \frac{b^{IG}}{RT} dP = 0 \xrightarrow[T=constant]{\{y_i\}_{i=1}^N=constant} \\ M \left(\frac{4\dot{m}}{M \cdot \pi \cdot D_p^2} \right)^2 \frac{b^{IG}}{RT} dV + M \left(\frac{2f}{D_p} \left(\frac{4\dot{m}}{M \cdot \pi \cdot D_p^2} \right)^2 V \right) \frac{b^{IG}}{RT} dl + d \left(\frac{Pb^{IG}}{RT} \right) = 0 \end{aligned}$$

Using the dimensionless variables $\beta^{IG} \triangleq \frac{Pb^{IG}}{RT}$, $\tilde{V}^{IG} \triangleq \frac{V}{b^{IG}}$ employed to create the DIGEOS

$\beta^{IG} = \frac{1}{\tilde{V}^{IG}}$, then yields the mechanical energy balance dimensionless differential form

$$\begin{aligned} \frac{Mb^{IG}}{RT} \left(\frac{4\dot{m}}{M \cdot \pi \cdot D_p^2} \right)^2 d(b^{IG} \tilde{V}^{IG}) + \frac{Mb^{IG}}{RT} \left(\frac{2f}{D_p} \left(\frac{4\dot{m}}{M \cdot \pi \cdot D_p^2} \right)^2 b^{IG} \tilde{V}^{IG} \right) d(L_p \tilde{l}) + d\beta^{IG} = 0 \xrightarrow[L_p=constant]{\{y_i\}_{i=1}^N=constant} \\ \frac{M(b^{IG})^2}{RT} \left(\frac{4\dot{m}}{M \cdot \pi \cdot D_p^2} \right)^2 d\tilde{V}^{IG} + \frac{M(b^{IG})^2}{RT} \left(\frac{2fL_p}{D_p} \left(\frac{4\dot{m}}{M \cdot \pi \cdot D_p^2} \right)^2 \tilde{V}^{IG} \right) d\tilde{l} + d \left(\frac{1}{\tilde{V}^{IG}} \right) = 0 \Rightarrow \\ \left[\frac{M(b^{IG})^2}{RT} \left(\frac{4\dot{m}}{M \cdot \pi \cdot D_p^2} \right)^2 - \frac{1}{(\tilde{V}^{IG})^2} \right] d\tilde{V}^{IG} + \frac{M(b^{IG})^2}{RT} \left(\frac{2fL_p}{D_p} \left(\frac{4\dot{m}}{M \cdot \pi \cdot D_p^2} \right)^2 \tilde{V}^{IG} \right) d\tilde{l} = 0 \Rightarrow \end{aligned}$$

$$\begin{aligned}
& - \left[\frac{M(b^{IG})^2}{RT} \left(\frac{4\dot{m}}{M \cdot \pi \cdot D_p^2} \right)^2 - \frac{1}{(\tilde{V}^{IG})^2} \right] d\tilde{V}^{IG} = d\tilde{l} \Rightarrow - \left[r_{KI}^{IG} - \frac{1}{(\tilde{V}^{IG})^2} \right] d\tilde{V}^{IG} = d\tilde{l} \Rightarrow \\
& \frac{M(b^{IG})^2}{RT} \left(\frac{2fL_p}{D_p} \left(\frac{4\dot{m}}{M \cdot \pi \cdot D_p^2} \right)^2 \tilde{V}^{IG} \right) \\
& \tilde{r}_0^{IG} \int_0^1 \left[\frac{-r_{LD}}{2f} \frac{1}{\tilde{V}^{IG}} + \frac{r_{LD}}{2f r_{KI}^{IG}} \left[\frac{1}{(\tilde{V}^{IG})^3} \right] \right] d\tilde{V}^{IG} = \int_0^1 d\tilde{l} = 1 \Rightarrow \\
& \left[- \left[\ln(\tilde{V}^{IG}(1)) - \ln(\tilde{V}_0^{IG}) \right] + \frac{1}{r_{KI}^{IG}} \left[-\frac{1}{2(\tilde{V}^{IG}(1))^2} + \frac{1}{2(\tilde{V}_0^{IG})^2} \right] \right] = \frac{2f}{r_{LD}}
\end{aligned}$$

Given the definitions

$$\gamma_1(\tilde{V}^{IG}) \triangleq -\ln(\tilde{V}^{IG}), \quad \gamma_2^{IG}(\tilde{V}^{IG}) \triangleq \frac{-1}{2(\tilde{V}^{IG})^2}, \quad \gamma^{IG}(\tilde{V}^{IG}) \triangleq \gamma_1(\tilde{V}^{IG}) + \frac{1}{r_{KI}^{IG}} \gamma_2^{IG}(\tilde{V}^{IG})$$

the above equation becomes:

$$\gamma^{IG}(\tilde{V}^{IG}(1)) - \gamma^{IG}(\tilde{V}_0^{IG}) \triangleq \left[\left[\gamma_1(\tilde{V}^{IG}(1)) + \frac{1}{r_{KI}^{IG}} \cdot \gamma_2^{IG}(\tilde{V}^{IG}(1)) \right] - \left[\gamma_1(\tilde{V}_0^{IG}) + \frac{1}{r_{KI}^{IG}} \cdot \gamma_2^{IG}(\tilde{V}_0^{IG}) \right] \right] = \frac{2f}{r_{LD}} \text{ OE}\Delta$$

b. GCEOS:

$$\begin{aligned}
& M \left(\frac{4\dot{m}}{M \cdot \pi \cdot D_p^2} \right)^2 dV + M \left(\frac{2f}{D_p} \left(\frac{4\dot{m}}{M \cdot \pi \cdot D_p^2} \right)^2 V \right) dl + dP = 0 \Rightarrow \\
& M \left(\frac{4\dot{m}}{M \cdot \pi \cdot D_p^2} \right)^2 \frac{b}{RT} dV + M \left(\frac{2f}{D_p} \left(\frac{4\dot{m}}{M \cdot \pi \cdot D_p^2} \right)^2 V \right) \frac{b}{RT} dl + \frac{b}{RT} dP = 0 \stackrel{T=constant}{\Rightarrow} \stackrel{\{y_i\}_{i=1}^N=constant}{=} \\
& M \left(\frac{4\dot{m}}{M \cdot \pi \cdot D_p^2} \right)^2 \frac{b}{RT} dV + M \left(\frac{2f}{D_p} \left(\frac{4\dot{m}}{M \cdot \pi \cdot D_p^2} \right)^2 V \right) \frac{b}{RT} dl + d \left(\frac{Pb}{RT} \right) = 0
\end{aligned}$$

and also using the dimensionless variables $\beta \triangleq \frac{Pb}{RT} > 0$, $q \triangleq \frac{a(T)}{bRT} > 0$, $\tilde{V} \triangleq \frac{V}{b}$ employed to

create DGCEOS, then yields the following dimensionless differential form of the mechanical energy balance:

$$\begin{aligned}
& \frac{Mb}{RT} \left(\frac{4\dot{m}}{M \cdot \pi \cdot D_p^2} \right)^2 d(b\tilde{V}) + \frac{Mb}{RT} \left(\frac{2f}{D_p} \left(\frac{4\dot{m}}{M \cdot \pi \cdot D_p^2} \right)^2 b\tilde{V} \right) d(L_p \tilde{l}) + d\beta = 0 \stackrel{L_p=constant}{\Rightarrow} \stackrel{\{y_i\}_{i=1}^N=constant}{=} \\
& \frac{Mb^2}{RT} \left(\frac{4\dot{m}}{M \cdot \pi \cdot D_p^2} \right)^2 d\tilde{V} + \frac{Mb^2}{RT} \left(\frac{2fL_p}{D_p} \left(\frac{4\dot{m}}{M \cdot \pi \cdot D_p^2} \right)^2 \tilde{V} \right) d\tilde{l} + \left[\frac{\partial \beta(q, \tilde{V})}{\partial \tilde{V}} d\tilde{V} + \frac{\partial \beta(q, \tilde{V})}{\partial q} dq \right] = 0 \stackrel{q=constant}{\Rightarrow}
\end{aligned}$$

$$\begin{aligned}
& \left[\frac{Mb^2}{RT} \left(\frac{4\dot{m}}{M \cdot \pi \cdot D_p^2} \right)^2 + \frac{\partial \beta(q, \tilde{V})}{\partial \tilde{V}} \right] d\tilde{V} + \frac{Mb^2}{RT} \left(\frac{2fL_p}{D_p} \left(\frac{4\dot{m}}{M \cdot \pi \cdot D_p^2} \right)^2 \tilde{V} \right) d\tilde{l} = 0 \Rightarrow \\
& - \left[\frac{Mb^2}{RT} \left(\frac{4\dot{m}}{M \cdot \pi \cdot D_p^2} \right)^2 + \frac{\partial \beta(q, \tilde{V})}{\partial \tilde{V}} \right] d\tilde{V} = d\tilde{l} \Rightarrow \\
& \frac{Mb^2}{RT} \left(\frac{2fL_p}{D_p} \left(\frac{4\dot{m}}{M \cdot \pi \cdot D_p^2} \right)^2 \tilde{V} \right) \\
& - \left[\frac{Mb^2}{RT} \left(\frac{4\dot{m}}{M \cdot \pi \cdot D_p^2} \right)^2 - \frac{1}{(\tilde{V}-1)^2} + \frac{q}{\sigma-\varepsilon} \left[\frac{1}{(\tilde{V}+\varepsilon)^2} - \frac{1}{(\tilde{V}+\sigma)^2} \right] \right] d\tilde{V} = d\tilde{l} \Rightarrow \\
& \frac{Mb^2}{RT} \left(\frac{2fL_p}{D_p} \left(\frac{4\dot{m}}{M \cdot \pi \cdot D_p^2} \right)^2 \tilde{V} \right) \\
& \left\{ \begin{array}{l} \left[r_{KI} + \frac{-1}{(\tilde{V}-1)^2} + \frac{q}{\sigma-\varepsilon} \left[\frac{1}{(\tilde{V}+\varepsilon)^2} - \frac{1}{(\tilde{V}+\sigma)^2} \right] \right] d\tilde{V} = d\tilde{l} \text{ if } \varepsilon \neq 0, \sigma \neq 0 \\ \left(\frac{2f\dot{r}_{KI}}{r_{LD}} \tilde{V} \right) \end{array} \right. \Rightarrow \\
& \left. \begin{array}{l} \left[r_{KI} + \frac{-1}{(\tilde{V}-1)^2} + \frac{q}{\sigma} \left[\frac{1}{(\tilde{V})^2} - \frac{1}{(\tilde{V}+\sigma)^2} \right] \right] d\tilde{V} = d\tilde{l} \text{ if } \varepsilon = 0, \sigma \neq 0 \\ \left(\frac{2f\dot{r}_{KI}}{r_{LD}} \tilde{V} \right) \end{array} \right\} \\
& \left\{ \begin{array}{l} \left[\frac{-r_{KI}}{\left(\frac{2f\dot{r}_{KI}}{r_{LD}} \tilde{V} \right)} + \frac{1}{(\tilde{V}-1)^2 \left(\frac{2f\dot{r}_{KI}}{r_{LD}} \tilde{V} \right)} - \frac{\frac{q}{\sigma-\varepsilon}}{(\tilde{V}+\varepsilon)^2 \left(\frac{2f\dot{r}_{KI}}{r_{LD}} \tilde{V} \right)} + \frac{\frac{q}{\sigma-\varepsilon}}{(\tilde{V}+\sigma)^2 \left(\frac{2f\dot{r}_{KI}}{r_{LD}} \tilde{V} \right)} \right] d\tilde{V} = d\tilde{l} \text{ if } \varepsilon \neq 0, \sigma \neq 0 \\ \left[\frac{-r_{KI}}{\left(\frac{2f\dot{r}_{KI}}{r_{LD}} \tilde{V} \right)} + \frac{1}{(\tilde{V}-1)^2 \left(\frac{2f\dot{r}_{KI}}{r_{LD}} \tilde{V} \right)} - \frac{\frac{q}{\sigma}}{(\tilde{V})^2 \left(\frac{2f\dot{r}_{KI}}{r_{LD}} \tilde{V} \right)} + \frac{\frac{q}{\sigma}}{(\tilde{V}+\sigma)^2 \left(\frac{2f\dot{r}_{KI}}{r_{LD}} \tilde{V} \right)} \right] d\tilde{V} = d\tilde{l} \text{ if } \varepsilon = 0, \sigma \neq 0 \end{array} \right\} \Rightarrow
\end{aligned}$$

Partial fraction expansion of the ratios that appear in the above differential form of the dimensionless mechanical energy balance yields:

$$\left\{ \begin{array}{l} \left[\frac{r_{LD}}{2f} \frac{-1}{\tilde{V}} + \frac{r_{LD}}{2fr_{KI}} \cdot \left[\frac{-\tilde{V}+2}{(\tilde{V}-1)^2} + \frac{1}{\tilde{V}} \right] - \frac{r_{LD}}{2fr_{KI}} \frac{q}{\sigma-\varepsilon} \left[\frac{-\tilde{V}-2\varepsilon}{\varepsilon^2 (\tilde{V}+\varepsilon)^2} + \frac{1}{\varepsilon^2 \tilde{V}} \right] + \right. \\ \left. + \frac{r_{LD}}{2fr_{KI}} \frac{q}{\sigma-\varepsilon} \left[\frac{-\tilde{V}-2\sigma}{\sigma^2 (\tilde{V}+\sigma)^2} + \frac{1}{\sigma^2 \tilde{V}} \right] \right] d\tilde{V} = d\tilde{l} \text{ if } \varepsilon \neq 0, \sigma \neq 0 \\ \\ \left[\frac{r_{LD}}{2f} \frac{-1}{\tilde{V}} + \frac{r_{LD}}{2fr_{KI}} \cdot \left[\frac{-\tilde{V}+2}{(\tilde{V}-1)^2} + \frac{1}{\tilde{V}} \right] - \frac{r_{LD}}{2fr_{KI}} \frac{q}{\sigma} \left[\frac{1}{\tilde{V}^3} \right] + \right. \\ \left. + \frac{r_{LD}}{2fr_{KI}} \frac{q}{\sigma} \left[\frac{-\tilde{V}-2\sigma}{\sigma^2 (\tilde{V}+\sigma)^2} + \frac{1}{\sigma^2 \tilde{V}} \right] \right] d\tilde{V} = d\tilde{l} \text{ if } \varepsilon = 0, \sigma \neq 0 \end{array} \right\}$$

Given the definitions

$$\left\{ \begin{array}{l} \gamma_1(\tilde{V}) \triangleq -\ln(\tilde{V}), \quad \gamma_2^{GC}(\tilde{V}) \triangleq \ln\left(\frac{\tilde{V}}{\tilde{V}-1}\right) - \frac{1}{(\tilde{V}-1)}, \\ \\ \gamma_3^{\varepsilon\sigma}(\tilde{V}) \triangleq \frac{-1}{\varepsilon^2(\sigma-\varepsilon)} \left[\ln\left(\frac{\tilde{V}}{\varepsilon+\tilde{V}}\right) + \frac{\varepsilon}{\varepsilon+\tilde{V}} \right] + \frac{1}{\sigma^2(\sigma-\varepsilon)} \left[\ln\left(\frac{\tilde{V}}{\sigma+\tilde{V}}\right) + \frac{\sigma}{\sigma+\tilde{V}} \right] \text{ if } \varepsilon \neq 0, \sigma \neq 0 \\ \\ \gamma_3^{0\sigma}(\tilde{V}) \triangleq \frac{1}{\sigma^2} \left[\frac{1}{\sigma} \ln\left(\frac{\tilde{V}}{\sigma+\tilde{V}}\right) + \frac{1}{\sigma+\tilde{V}} \right] + \frac{1}{2\sigma(\tilde{V})^2} \text{ if } \varepsilon = 0, \sigma \neq 0 \\ \\ \gamma^{\varepsilon\sigma}(\tilde{V}) \triangleq \left[\gamma_1(\tilde{V}) + \frac{1}{r_{KI}} \cdot \gamma_2^{GC}(\tilde{V}) + \frac{q}{r_{KI}} \cdot \gamma_3^{\varepsilon\sigma}(\tilde{V}) \right] \text{ if } \varepsilon \neq 0, \sigma \neq 0 \\ \\ \gamma^{0\sigma}(\tilde{V}) \triangleq \left[\gamma_1(\tilde{V}) + \frac{1}{r_{KI}} \cdot \gamma_2^{GC}(\tilde{V}) + \frac{q}{r_{KI}} \cdot \gamma_3^{0\sigma}(\tilde{V}) \right] \text{ if } \varepsilon = 0, \sigma \neq 0 \end{array} \right\},$$

the integration of the above differential form of the dimensionless mechanical energy balance along the dimensionless pipeline length then yields:

For $\varepsilon \neq 0, \sigma \neq 0$:

$$\int_{\tilde{V}_0}^{\tilde{V}(1)} \left[\frac{-r_{LD}}{2f} \frac{1}{\tilde{V}} + \frac{r_{LD}}{2fr_{KI}} \cdot \left[\frac{-\tilde{V}+2}{(\tilde{V}-1)^2} + \frac{1}{\tilde{V}} \right] - \frac{r_{LD}}{2fr_{KI}} \frac{q}{\varepsilon^2(\sigma-\varepsilon)} \left[\frac{-\tilde{V}-2\varepsilon}{(\tilde{V}+\varepsilon)^2} + \frac{1}{\tilde{V}} \right] + \right. \\ \left. + \frac{r_{LD}}{2fr_{KI}} \frac{q}{\sigma^2(\sigma-\varepsilon)} \left[\frac{-\tilde{V}-2\sigma}{(\tilde{V}+\sigma)^2} + \frac{1}{\tilde{V}} \right] \right] d\tilde{V} = \int_0^1 d\tilde{l} = 1 \stackrel{[Wol24a]}{\Rightarrow} \stackrel{[Wol24b]}{=}$$

$$\begin{aligned}
& \left[\frac{-r_{LD}}{2f} \left[\ln(\tilde{V}(1)) - \ln(\tilde{V}_0) \right] + \frac{r_{LD}}{2fr_{KI}} \cdot \left[\left[-\ln(\tilde{V}(1)-1) - \frac{1}{(\tilde{V}(1)-1)} \right] - \left[-\ln(\tilde{V}_0-1) - \frac{1}{(\tilde{V}_0-1)} \right] + \ln(\tilde{V}(1)) - \ln(\tilde{V}_0) \right] - \right. \\
& \left. - \frac{r_{LD}}{2fr_{KI}} \frac{q}{\varepsilon^2(\sigma-\varepsilon)} \left[\left[-\ln(\varepsilon+\tilde{V}(1)) + \frac{\varepsilon}{\varepsilon+\tilde{V}(1)} \right] - \left[-\ln(\varepsilon+\tilde{V}_0) + \frac{\varepsilon}{\varepsilon+\tilde{V}_0} \right] + \left[\ln(\tilde{V}(1)) - \ln(\tilde{V}_0) \right] \right] + \right. \\
& \left. + \frac{r_{LD}}{2fr_{KI}} \frac{q}{\sigma^2(\sigma-\varepsilon)} \left[\left[-\ln(\sigma+\tilde{V}(1)) + \frac{\sigma}{\sigma+\tilde{V}(1)} \right] - \left[-\ln(\sigma+\tilde{V}_0) + \frac{\sigma}{\sigma+\tilde{V}_0} \right] + \left[\ln(\tilde{V}(1)) - \ln(\tilde{V}_0) \right] \right] \right] = 1 \Rightarrow \\
& \left[\left[\ln(\tilde{V}(1)) - \ln(\tilde{V}_0) \right] + \frac{1}{r_{KI}} \cdot \left[\left[-\ln(\tilde{V}(1)-1) - \frac{1}{(\tilde{V}(1)-1)} \right] - \left[-\ln(\tilde{V}_0-1) - \frac{1}{(\tilde{V}_0-1)} \right] + \ln(\tilde{V}(1)) - \ln(\tilde{V}_0) \right] - \right. \\
& \left. - \frac{1}{r_{KI}} \frac{q}{\varepsilon^2(\sigma-\varepsilon)} \left[\left[-\ln(\varepsilon+\tilde{V}(1)) + \frac{\varepsilon}{\varepsilon+\tilde{V}(1)} \right] - \left[-\ln(\varepsilon+\tilde{V}_0) + \frac{\varepsilon}{\varepsilon+\tilde{V}_0} \right] + \left[\ln(\tilde{V}(1)) - \ln(\tilde{V}_0) \right] \right] + \right. \\
& \left. + \frac{1}{r_{KI}} \frac{q}{\sigma^2(\sigma-\varepsilon)} \left[\left[-\ln(\sigma+\tilde{V}(1)) + \frac{\sigma}{\sigma+\tilde{V}(1)} \right] - \left[-\ln(\sigma+\tilde{V}_0) + \frac{\sigma}{\sigma+\tilde{V}_0} \right] + \left[\ln(\tilde{V}(1)) - \ln(\tilde{V}_0) \right] \right] \right] = \frac{2f}{r_{LD}} \Rightarrow \\
& \boxed{\gamma^{\varepsilon\sigma}(\tilde{V}(1)) - \gamma^{\varepsilon\sigma}(\tilde{V}_0) \triangleq \left[\left[\gamma_1(\tilde{V}(1)) + \frac{1}{r_{KI}} \cdot \gamma_2^{GC}(\tilde{V}(1)) + \frac{q}{r_{KI}} \cdot \gamma_3^{\varepsilon\sigma}(\tilde{V}(1)) \right] - \right.} \\
& \left. \left[\left[\gamma_1(\tilde{V}_0) + \frac{1}{r_{KI}} \cdot \gamma_2^{GC}(\tilde{V}_0) + \frac{q}{r_{KI}} \cdot \gamma_3^{\varepsilon\sigma}(\tilde{V}_0) \right] \right] = \frac{2f}{r_{LD}} \text{ if } \varepsilon \neq 0, \sigma \neq 0}
\end{aligned}$$

For $\varepsilon = 0, \sigma \neq 0$:

$$\begin{aligned}
& \int_{\tilde{V}_0}^{\tilde{V}(1)} \left[\frac{-r_{LD}}{2f} \frac{1}{\tilde{V}} + \frac{r_{LD}}{2fr_{KI}} \cdot \left[\frac{-\tilde{V}+2}{(\tilde{V}-1)^2} + \frac{1}{\tilde{V}} \right] - \frac{r_{LD}}{2fr_{KI}} \frac{q}{\sigma} \left[\frac{1}{\tilde{V}^3} \right] + \frac{r_{LD}}{2fr_{KI}} \frac{q}{\sigma^3} \left[\frac{-\tilde{V}-2\sigma}{(\tilde{V}+\sigma)^2} + \frac{1}{\tilde{V}} \right] \right] d\tilde{V} = \int_0^1 d\tilde{l} = 1 \Rightarrow \\
& \left[\left[\ln(\tilde{V}(1)) - \ln(\tilde{V}_0) \right] + \frac{1}{r_{KI}} \cdot \left[\left[-\ln(\tilde{V}(1)-1) - \frac{1}{(\tilde{V}(1)-1)} \right] - \left[-\ln(\tilde{V}_0-1) - \frac{1}{(\tilde{V}_0-1)} \right] + \ln(\tilde{V}(1)) - \ln(\tilde{V}_0) \right] - \right. \\
& \left. - \frac{1}{r_{KI}} \frac{q}{\sigma} \left[-\frac{1}{2(\tilde{V}(1))^2} + \frac{1}{2(\tilde{V}_0)^2} \right] + \right. \\
& \left. + \frac{1}{r_{KI}} \frac{q}{\sigma^3} \left[\left[-\ln(\sigma+\tilde{V}(1)) + \frac{\sigma}{\sigma+\tilde{V}(1)} \right] - \left[-\ln(\sigma+\tilde{V}_0) + \frac{\sigma}{\sigma+\tilde{V}_0} \right] + \left[\ln(\tilde{V}(1)) - \ln(\tilde{V}_0) \right] \right] \right] = \frac{2f}{r_{LD}} \Rightarrow \\
& \boxed{\gamma^{0\sigma}(\tilde{V}(1)) - \gamma^{0\sigma}(\tilde{V}_0) \triangleq \left[\left[\gamma_1(\tilde{V}(1)) + \frac{1}{r_{KI}} \cdot \gamma_2^{GC}(\tilde{V}(1)) + \frac{q}{r_{KI}} \cdot \gamma_3^{0\sigma}(\tilde{V}(1)) \right] - \right.} \\
& \left. \left[\left[\gamma_1(\tilde{V}_0) + \frac{1}{r_{KI}} \cdot \gamma_2^{GC}(\tilde{V}_0) + \frac{q}{r_{KI}} \cdot \gamma_3^{0\sigma}(\tilde{V}_0) \right] \right] = \frac{2f}{r_{LD}} \text{ if } \varepsilon = 0, \sigma \neq 0 \text{ O.E.}\Delta.}
\end{aligned}$$

A.2. Case Study 1 CH₄-H₂ mix viscosity equation analysis:

$$\begin{aligned}
\mu(T) &= \frac{y_{H_2} \mu_{H_2}(T)}{y_{H_2} \Phi_{H_2, H_2}(T) + y_{CH_4} \Phi_{H_2, CH_4}(T)} + \frac{y_{CH_4} \mu_{CH_4}(T)}{y_{H_2} \Phi_{CH_4, H_2}(T) + y_{CH_4} \Phi_{CH_4, CH_4}(T)} \xrightarrow{\Phi_{H_2, H_2}(T)=1} \\
\mu(T) &= \frac{y_{H_2} \mu_{H_2}(T)}{y_{H_2} + (1-y_{H_2}) \Phi_{H_2, CH_4}(T)} + \frac{(1-y_{H_2}) \mu_{CH_4}(T)}{y_{H_2} \Phi_{CH_4, H_2}(T) + (1-y_{H_2})} \Rightarrow \\
\mu(T) &= \frac{y_{H_2} \mu_{H_2}(T)}{\Phi_{H_2, CH_4}(T) + y_{H_2} (1-\Phi_{H_2, CH_4}(T))} + \frac{(1-y_{H_2}) \mu_{CH_4}(T)}{1 + y_{H_2} (\Phi_{CH_4, H_2}(T)-1)} \Rightarrow \\
\mu(T) &= \frac{\left[y_{H_2} \mu_{H_2}(T) \left[1 + y_{H_2} (\Phi_{CH_4, H_2}(T)-1) \right] + \right.}{\left[\Phi_{H_2, CH_4}(T) + y_{H_2} (1-\Phi_{H_2, CH_4}(T)) \right] \left[1 + y_{H_2} (\Phi_{CH_4, H_2}(T)-1) \right]} \Rightarrow \\
&\quad \left. + (1-y_{H_2}) \mu_{CH_4}(T) \left[\Phi_{H_2, CH_4}(T) + y_{H_2} (1-\Phi_{H_2, CH_4}(T)) \right] \right] \\
\mu(T) &= \frac{\left[\left[\mu_{CH_4}(T) \Phi_{H_2, CH_4}(T) \right] + \left[\begin{array}{l} \mu_{H_2}(T) - \mu_{CH_4}(T) \Phi_{H_2, CH_4}(T) + \\ + \mu_{CH_4}(T) (1-\Phi_{H_2, CH_4}(T)) \end{array} \right] y_{H_2} + \right.}{\left[\Phi_{H_2, CH_4}(T) + y_{H_2} (1-\Phi_{H_2, CH_4}(T)) \right] \left[1 + y_{H_2} (\Phi_{CH_4, H_2}(T)-1) \right]} \Rightarrow \\
&\quad \left. + \left[\begin{array}{l} \mu_{H_2}(T) (\Phi_{CH_4, H_2}(T)-1) - \\ - \mu_{CH_4}(T) (1-\Phi_{H_2, CH_4}(T)) \end{array} \right] y_{H_2}^2 \right] \\
\mu(T) &= \frac{\left[\left[\mu_{CH_4}(T) \Phi_{H_2, CH_4}(T) \right] + \left[\begin{array}{l} \mu_{H_2}(T) + \mu_{CH_4}(T) - \\ - 2\mu_{CH_4}(T) \Phi_{H_2, CH_4}(T) \end{array} \right] y_{H_2} + \right.}{\left[\Phi_{H_2, CH_4}(T) + y_{H_2} (1-\Phi_{H_2, CH_4}(T)) \right] \left[1 + y_{H_2} (\Phi_{CH_4, H_2}(T)-1) \right]} \Rightarrow \\
&\quad \left. + \left[\begin{array}{l} \mu_{H_2}(T) (\Phi_{CH_4, H_2}(T)-1) + \\ + \mu_{CH_4}(T) (\Phi_{H_2, CH_4}(T)-1) \end{array} \right] y_{H_2}^2 \right]
\end{aligned}$$

Considering $\mu(T)$: $y_{H_2} \rightarrow \mu(T)(y_{H_2})$ as a function of y_{H_2} , then yields that the derivative

$$\frac{d\mu(T)}{dy_{H_2}} : y_{H_2} \rightarrow \frac{d\mu(T)}{dy_{H_2}}(y_{H_2}) \text{ is:}$$

$$\frac{d\mu(T)}{dy_{H_2}}(y_{H_2}) = \frac{\left[\begin{array}{l} \left[\begin{array}{l} \mu_{H_2}(T) + \mu_{CH_4}(T) - \\ - 2\mu_{CH_4}(T)\Phi_{H_2,CH_4}(T) \end{array} \right] \Phi_{H_2,CH_4}(T) - \\ - \left[\begin{array}{l} \mu_{CH_4}(T)\Phi_{H_2,CH_4}(T) \end{array} \right] (1 - \Phi_{H_2,CH_4}(T)) - \\ - \left[\begin{array}{l} \mu_{CH_4}(T)\Phi_{H_2,CH_4}(T) \end{array} \right] \Phi_{H_2,CH_4}(T)(\Phi_{CH_4,H_2}(T) - 1) \end{array} \right] + \\ + 2 \left[\begin{array}{l} \left[\begin{array}{l} \mu_{H_2}(T)(\Phi_{CH_4,H_2}(T) - 1) + \\ + \mu_{CH_4}(T)(\Phi_{H_2,CH_4}(T) - 1) \end{array} \right] \Phi_{H_2,CH_4}(T) - \\ - \left[\begin{array}{l} \mu_{CH_4}(T)\Phi_{H_2,CH_4}(T) \end{array} \right] (1 - \Phi_{H_2,CH_4}(T))(\Phi_{CH_4,H_2}(T) - 1) \end{array} \right] y_{H_2} + \\ + \left[\begin{array}{l} \left[\begin{array}{l} \mu_{H_2}(T)(\Phi_{CH_4,H_2}(T) - 1) + \\ + \mu_{CH_4}(T)(\Phi_{H_2,CH_4}(T) - 1) \end{array} \right] (1 - \Phi_{H_2,CH_4}(T)) + \\ + \left[\begin{array}{l} \mu_{H_2}(T)(\Phi_{CH_4,H_2}(T) - 1) + \\ + \mu_{CH_4}(T)(\Phi_{H_2,CH_4}(T) - 1) \end{array} \right] \Phi_{H_2,CH_4}(T)(\Phi_{CH_4,H_2}(T) - 1) - \\ - \left[\begin{array}{l} \mu_{H_2}(T) + \mu_{CH_4}(T) - \\ - 2\mu_{CH_4}(T)\Phi_{H_2,CH_4}(T) \end{array} \right] (1 - \Phi_{H_2,CH_4}(T))(\Phi_{CH_4,H_2}(T) - 1) \end{array} \right] y_{H_2}^2 \end{array} \right] }{\left[\Phi_{H_2,CH_4}(T) + y_{H_2}(1 - \Phi_{H_2,CH_4}(T)) \right]^2 \left[1 + y_{H_2}(\Phi_{CH_4,H_2}(T) - 1) \right]^2}$$

For case study 1, substituting:

$$\left. \begin{array}{l} \mu_{H_2}(T) = 8.9190 \cdot 10^{-6} \left(\frac{kg H_2}{m \cdot s} \right) \\ \mu_{CH_4}(T) = 1.0741 \cdot 10^{-5} \left(\frac{kg H_2}{m \cdot s} \right) \\ \Phi_{H_2,CH_4}(T) = \frac{\left[1 + \left(8.9190 \cdot 10^{-6} / 1.0741 \cdot 10^{-5} \right)^{1/2} \cdot \left(16.043 \cdot 10^{-3} / 2.016 \cdot 10^{-3} \right)^{1/4} \right]^2}{\left[8 \left(1 + \left(2.016 \cdot 10^{-3} / 16.043 \cdot 10^{-3} \right) \right)^{1/2} \right]^2} = 2.1338 \\ \Phi_{CH_4,H_2}(T) = \frac{\left[1 + \left(1.0741 \cdot 10^{-5} / 8.9190 \cdot 10^{-6} \right)^{1/2} \cdot \left(2.016 \cdot 10^{-3} / 16.043 \cdot 10^{-3} \right)^{1/4} \right]^2}{\left[8 \left(1 + \left(16.043 \cdot 10^{-3} / 2.016 \cdot 10^{-3} \right) \right)^{1/2} \right]^2} = 0.32292 \end{array} \right\}$$

$$\frac{d\mu(T)}{dy_{H_2}}(y_{H_2}) = \frac{\left[\begin{array}{l} \left[8.9190 \cdot 10^{-6} + 1.0741 \cdot 10^{-5} - \right] \cdot 2.1338 - \\ - 2 \cdot 1.0741 \cdot 10^{-5} \cdot 2.1338 \\ - \left[1.0741 \cdot 10^{-5} \cdot 2.1338 \right] (1 - 2.1338) - \\ - \left[1.0741 \cdot 10^{-5} \cdot 2.1338 \right] \cdot 2.1338 (0.32292 - 1) \end{array} \right] + \right. \\ \left. + 2 \left[\begin{array}{l} \left[8.9190 \cdot 10^{-6} (0.32292 - 1) + \right] \cdot 2.1338 - \\ + 1.0741 \cdot 10^{-5} (2.1338 - 1) \\ - \left[1.0741 \cdot 10^{-5} \cdot 2.1338 \right] (1 - 2.1338) (0.32292 - 1) \end{array} \right] y_{H_2} + \right. \\ \left. + \left[\begin{array}{l} \left[8.9190 \cdot 10^{-6} (0.32292 - 1) + \right] (1 - 2.1338) + \\ + 1.0741 \cdot 10^{-5} (2.1338 - 1) \end{array} \right] \\ + \left[\begin{array}{l} \left[8.9190 \cdot 10^{-6} (0.32292 - 1) + \right] 2.1338 (0.32292 - 1) - \\ - \left[8.9190 \cdot 10^{-6} + 1.0741 \cdot 10^{-5} - \right] (1 - 2.1338) (0.32292 - 1) \end{array} \right] y_{H_2}^2 \right] \\ \left. \frac{d\mu(T)}{dy_{H_2}}(y_{H_2}) \right] \Rightarrow$$

$$\frac{d\mu(T)}{dy_{H_2}}(y_{H_2}) = \frac{\left[3.2384 \cdot 10^{-6} - 8.9879 \cdot 10^{-6} y_{H_2} + 4.2656 \cdot 10^{-6} y_{H_2}^2 \right]}{\left[2.1338 - 1.1338 y_{H_2} \right]^2 \left[1 - 0.6771 y_{H_2} \right]^2}$$

$$\left\{ \frac{d\mu(T)}{dy_{H_2}}(y_{H_2}) \geq 0 \wedge y_{H_2} \in [0,1] \right\} \Leftrightarrow$$

$$\left\{ 4.2656 \cdot 10^{-6} y_{H_2}^2 - 8.9879 \cdot 10^{-6} y_{H_2} + 3.2384 \cdot 10^{-6} \geq 0 \wedge y_{H_2} \in [0,1] \right\} \Leftrightarrow$$

$$\left\{ y_{H_2}^2 - \frac{8.9879}{4.2656} y_{H_2} + \frac{3.2384}{4.2656} \geq 0 \wedge y_{H_2} \in [0,1] \right\} \Leftrightarrow$$

$$\left\{ \begin{array}{l} y_{H_2} \geq \frac{1}{2} \left(\frac{8.9879}{4.2656} + \sqrt{\left(\frac{8.9879}{4.2656} \right)^2 - 4 \frac{3.2384}{4.2656}} \right) \vee \\ y_{H_2} \leq \frac{1}{2} \left(\frac{8.9879}{4.2656} - \sqrt{\left(\frac{8.9879}{4.2656} \right)^2 - 4 \frac{3.2384}{4.2656}} \right) \end{array} \right\} \wedge y_{H_2} \in [0,1] \Leftrightarrow$$

$$\left\{ \left\{ y_{H_2} \geq 1.6458 \vee y_{H_2} \leq 0.4613 \right\} \wedge y_{H_2} \in [0,1] \right\} \Rightarrow y_{H_2} \in [0, 0.4613] \text{ O.E.Δ}$$